INFORMATION TO USERS

This manuscript has been reproduced from the microfilm master. UMI films the text directly from the original or copy submitted. Thus, some thesis and dissertation copies are in typewriter face, while others may be from any type of computer printer.

The quality of this reproduction is dependent upon the quality of the copy submitted. Broken or indistinct print, colored or poor quality illustrations and photographs, print bleedthrough, substandard margins, and improper alignment can adversely affect reproduction.

In the unlikely event that the author did not send UMI a complete manuscript and there are missing pages, these will be noted. Also, if unauthorized copyright material had to be removed, a note will indicate the deletion.

Oversize materials (e.g., maps, drawings, charts) are reproduced by sectioning the original, beginning at the upper left-hand corner and continuing from left to right in equal sections with small overlaps.

Photographs included in the original manuscript have been reproduced xerographically in this copy. Higher quality 6" x 9" black and white photographic prints are available for any photographs or illustrations appearing in this copy for an additional charge. Contact UMI directly to order.

Bell & Howell Information and Learning
300 North Zeeb Road, Ann Arbor, MI 48106-1346 USA
800-521-0600

UMI®

Université d'Ottawa • University of Ottawa

IMPLEMENTATION OF POWER AND FORCE ADAPTIVE CONTROL OF THE END MILLING PROCESS

THESIS

Submitted to the School of Graduate Studies and Research of the University of Ottawa in partial fulfilment of the requirements for the Degree of Master of Applied Science

By

Zhixin Han

Department of Mechanical Engineering

University of Ottawa

Ottawa, Ontario, Canada

National Library of Canada
Acquisitions and Bibliographic Services
395 Wellington Street
Ottawa ON K1A 0N4
Canada

Bibliothèque nationale du Canada
Acquisitions et services bibliographiques
395, rue Wellington
Ottawa ON K1A 0N4
Canada

Your file Votre référence

Our file Notre référence

0-612-46583-7

Canada

To my parents

Acknowledgements

I would like to express my sincere gratitude to my supervisor Dr. M. Liang and co-supervisor Dr. T. Yeap for their continued guidance and efforts throughout this thesis. The technical assistance of Madan Makasare, Mike Burns and Kola Porubovich is also gratefully acknowledged.

I would also like to thank the members of my defence committee Dr. D.S. Necsulescu and Dr. M.J. McDill for sparing their time and efforts in examining my thesis.

My special thanks go to my friend Pauline and my family for their continued support and encouragement.

Table of Contents

List of Figures

List of Tables

Nomenclature

a	Axial depth of cut
A	Denominator of process model, $A(z^{-1}) = 1+a_1z^{-1}+a_2z^{-2}+\cdots+a_{n_a}z^{-n_a}$
A_m	Denominator of reference model
b	Compensation factor in the DB MRAC
B	Numerator of process model, $B(z^{-1}) = b_0+b_1z^{-1}+b_2z^{-2}+\cdots+b_{n_b}z^{-n_b}$
B_m	Numerator of reference model
B_v	Viscous damping coefficient
C_r	Regulation dynamics polynomial, $C_r(z^{-1}) = 1+c_1z^{-1}+c_2z^{-2}+\cdots$
d	Time delay step
e	Input error
f_{act}	Actual feedrate
F_c	Cutting force
$\overline{F}_c$	Average cutting force
f_{cmd}	Command feedrate
F_x	X (table) component of cutting force
F_y	Y (cross) component of cutting force
G_c	Transfer function of controller
G_{cp}	Transfer function of cutting process
G_{fd}	Transfer function of feed drive system

G_p Transfer function of end milling process

G_{sp} Transfer function of spindle system

I Unit matrix

k Control interval counter

K System gain

K_{cp} Gain of cutting process

K_{fd} Gain of feed drive system

K_{ft} Force-to-torque gain

K_{sp} Gain of spindle system

m Fractional time delay step

n_a Order of process numerator $A(z^{-1})$

n_b Order of process denominator $B(z^{-1})$

n_c Order of regulation dynamics $C_r(z^{-1})$

n_s Spindle-to-motor ratio

P Covariance matrix

P_g Rotor input power

P_s Spindle power

$\overline{P}_s$ Average spindle power

Q Normalization parameter in the modified MRAC

R Controller parameter polynomial, $R(z^{-1}) = r_0 + r_1 z^{-1} + r_2 z^{-2} + \cdots$

s LaPlace transform operator

S Controller parameter polynomial, $S(z^{-1}) = 1 + s_1 z^{-1} + s_2 z^{-2} + \cdots$

T	Control interval
T_c	Cutting torque
T_e	Output torque of spindle motor
T_f	Coulomb friction
u	Process input
y	Process output
y_m	Reference model output
y_{ref}	Output reference
z	Forward-shift operator
α	Covariance matrix resetting factor
δ	Delay time
Δ	Denotation of changes
ε	Tracking error
θ	Estimated parameter vector
λ	Forgetting factor
λ_0	Factor for discarding initial data
τ	System time constant
τ_{cp}	Time constant of cutting process
ϕ	Input and output vector
ω_m	Angular speed of spindle motor
ω_s	Synchronous speed of spindle motor

Abstract

This thesis explores the application of adaptive control for power and force control in the end milling process. The spindle power and cutting force are maintained at desired levels despite the variations in the depth of cut and the workpiece properties.

A first-order discrete model is used to represent the relationship between the process output (spindle power or cutting force) and the feedrate input. By open-loop experiments, the model is validated and the process parameters of the spindle power and cutting force systems are identified. The process is found to have pure time delay and can be a non-minimum phase system. A Deadbeat (DB) Model Reference Adaptive Control (MRAC) algorithm is compared with modified MRAC, a typical scheme in existing adaptive control systems for non-minimum phase end milling processes. The design of the two controllers is described and simulations are presented. It is shown that the DB MRAC has less design complexity and superior control performance in simulation studies than the modified MRAC. Actual cutting tests of spindle power and cutting force control in the end milling process using the DB MRAC algorithm are carried out for a variety of cutting conditions. The control systems are stable with good transient and steady-state performance. The successful experimental results demonstrate the effectiveness of the DB MRAC scheme for spindle power and cutting force control of the end milling process and the feasibility of spindle power control in adaptive control of end milling processes.

Chapter 1

Introduction

1.1 Background

In manufacturing, machining operations such as turning, milling, drilling and grinding are widely used and mature technologies dating back to 18th century. The objective of improving production rate while maintaining high product quality has resulted in many improvements in machines, cutting tools, and materials. The introduction of Numerically Controlled (NC) machine tools by Parson's Machine Tool Company (Michigan, USA) in 1950's was one of the most important developments. In the last two decades, as computers became cheaper, more powerful and reliable, the servo-control function was implemented on computers instead of hard-wired digital circuits. Thus Computer Numerically Controlled (CNC) machine tools were introduced, bringing improvements in system flexibility and part programming.

NC/CNC machine tools have provided significant improvements in productivity and greatly reduced operator input. However, one of the main limitations of current NC and CNC machine tools is that the machine operating parameters, such as feedrates and spindle speeds, need to be preset and are fixed throughout the operation. Since these parameters are selected based on the most severe conditions expected, conservative

feedrate and spindle speed values are usually used, which consequently slow down the system production. Therefore, over the last two decades, there has been an increasing interest in implementing a higher level process control aiming at improving production rates and product quality. Many adaptive control systems have been developed which automatically manipulate the machining parameters and adapt the controller gains or parameters to changes in the machining process such as depth of cut and material properties, so as to maintain acceptable control performance despite the changes (Ulsoy et al., 1983). These systems were investigated and implemented on various machining operations such as turning, milling and grinding, etc.

1.2 Motivation

Great progress has been made in the development and implementation of adaptive control systems for maintaining a constant cutting load in end milling processes. Various adaptive control approaches have been proposed. However, in the literature, only force control has been extensively investigated and no attempt has been made to develop adaptive power control systems for end milling processes. Only cases where the process has insignificant output time delay and thus can be modelled as a minimum phase system have been studied in depth (Barthel and Shin, 1993).

Force control of end milling processes is impractical which leads to poor industrial acceptance of existing adaptive control systems. Firstly, force sensors are generally mounted on the table. This complex mounting affects the dynamics of the machine tool structure. Secondly, the dynamometers are usually directly exposed to the

severe machining environment and thus could be ruined by fluid, chips and possible overload. Furthermore, multi-dimensional force sensors, which are usually used in force control approaches, are very expensive (e.g., the Kistler 9257B 3-component dynamometer used in this thesis costs about $35,000). Instead, spindle power control seems to be a promising alternative for adaptive control of end milling processes. Spindle power is linearly related to motor speed and cutting load. In addition, at typical spindle speeds used practically, the spindle system has sufficient bandwidth capacities and sensitivity for monitoring the cutting load (Stein and Wang, 1990). The delay of the power signal will not be comparably longer than that of the force signal because in general, commercially used machine tools are equipped with spindle systems that are highly responsive (Stein and Wang, 1990). In such scheme, the system setup is simple and the power sensor is not exposed to the cutting environment. Since the power is measured from the power supply, the dynamics of the machine tool are not affected. Also power sensors are much cheaper than force sensors (it costs about $1000 dollars for the Load Controls PH-3A power sensor used in this thesis).

In end milling process control, there is always a time delay caused by, for example, the implementation of input commands and the measurement of output signals. As pointed out by researchers (Liu and Liang, 1989; Kim and Huang, 1992), it is common for an end milling process to behave as non-minimum phase system when the process time delay is significant compared with the sampling interval. Most adaptive control schemes discussed in the literature are for minimum phase systems so that they are not directly applicable to non-minimum phase systems. A few adaptive control

approaches, including the modified MRAC (Liu and Liang, 1989), the modified quasi-direct MRAC (Barthel and Shin, 1993) and the pole-placement adaptive controller (Kim and Huang, 1992), have been proposed in the last several years to cope with non-minimum phase end milling processes. The drawback of these indirect adaptive control schemes is that the complexity of design and implementation increases and the control performance degrades with the order of process model (Baker and Morris, 1985). Therefore, development of adaptive controllers that are simple to design and implement and can perform well under a large variety of cutting conditions for end milling processes, especially non-minimum phase end milling processes, is still needed.

1.3 Objective and Proposed Approach

The objective of this thesis is to develop an effective adaptive control scheme for end milling processes and examine the practicability of power control in end milling process adaptive control. The end milling process to be studied has a long time delay and is likely to be a non-minimum phase plant. Constant power control is the main concern. Constant force control will also be discussed for the purpose of comparison. The developed systems should maintain the desired constant spindle power and cutting force levels by adjusting the feedrate automatically in the presence of time-varying cutting conditions. Such conditions would be sudden changes in the depth of cut or changes in workpiece properties.

To accomplish this goal, the following work is carried out in this thesis:

1. An end milling system model is developed based on dynamic analysis of the

process. The established model is then verified and the parameters of the discrete process model are identified by open-loop cutting experiments.

2. Two adaptive algorithms capable of controlling non-minimum phase processes, the Deadbeat Model Reference Adaptive Controller(DB MRAC) and the modified MRAC, are evaluated by simulation of power and force control of the end milling process. An explicit Recursive Least Square (RLS) parameter estimation scheme using both covariance matrix resetting and a variable forgetting factor is used for on-line identification of the process parameters.
3. Actual machining tests of spindle power and cutting force control are conducted to evaluate the effectiveness of the DB MRAC scheme under a variety of cutting conditions.

1.4 Thesis Overview

The remainder of the thesis is divided into five chapters. Chapter 2 includes a brief review of adaptive control theory and previous research work on adaptive control of machining processes. In Chapter 3, the modelling of the end milling process is discussed. The process parameters are identified for simulation studies. Chapter 4 elaborates the simulation evaluation of the DB MRAC and modified MRAC schemes. In Chapter 5, the experimental results of applying the DB MRAC scheme to spindle power and cutting force control of the end milling process are presented. Finally, Chapter 6 gives the conclusions of this research and some recommendations for future research.

Chapter 2

Adaptive Control of Machining Processes

This chapter introduces general adaptive control theory and reviews the developments in adaptive control of machining processes.

2.1 General Adaptive Control Theory

In the development of modern control theory, it was realized that a fixed gain, linear feedback controller cannot provide acceptable system performance for all situations, particularly when the process to be controlled has unknown or time-varying parameters. Thus there was extensive research on adaptive control in the 1950's, starting with the development of the gain-scheduling technique (Astrom and Wittenmark, 1989). Due to the developments in system identification and control theory, adaptive control theory has developed rapidly in the last two decades. Now there is an established theoretical basis for the design of adaptive controllers. Adaptive control has been used in process control, robotics, aerospace and other industrial control systems.

Among the many different approaches to adaptive control proposed in the literature, the Model Reference Adaptive Controller (MRAC) and the Self-Tuning Controller (STC) are two common schemes. In the following subsections, the basic

design concepts and control structure of these two approaches will be presented.

2.1.1 Model Reference Adaptive Controller (MRAC)

Figure 2.1 shows a parallel MRAC, the most popular form. In this scheme, an ordinary controller is used to obtain suitable closed-loop behaviour, as in non-adaptive control schemes. The desired process response to a command signal is specified by means of a reference model. An adaption mechanism keeps track of the process output y and the model output y_m and calculates a suitable controller parameter setting such that the difference between these outputs tends to zero. In addition to the process output y and input u, the process states, or the reference signal y_{ref}, may be used by the adaption mechanism.

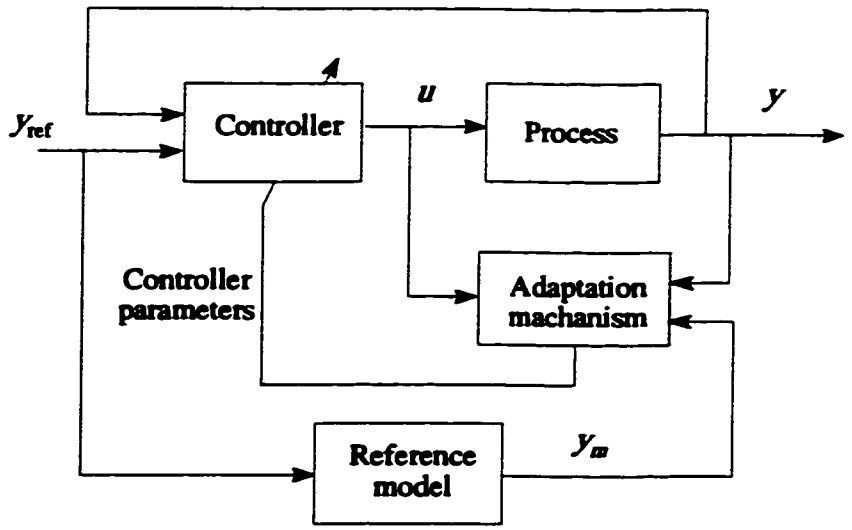

Figure 2.1 Block diagram of parallel MRAC

In Figure 2.1, the reference model is placed in parallel with the process. There are many alternatives (Landau, 1979), of which the series type MRAC is the most well known. In this scheme, the reference model is placed in cascade with the process and can be regarded as a trajectory generator which specifies an achievable process response. In other adaptive control schemes, such as the STC or the predictive adaptive control, a series-type reference model is also used, and is called a reference generator (Astrom and Wittenmark, 1989).

Adaptive law design is an important issue in MRAC. The sensitivity model (MIT rule) was first used and the stability theory of Lyapunov and Popov's hyperstability theory served as standard design methods later (Astrom and Wittenmark, 1989). Some modern discrete-time MRAC algorithms allow separate specification of the tracking and regulation requirements. These algorithms have a strong resemblance to the STC schemes, and some can be shown to be equivalent (Egardt, 1980).

2.1.2 Self-Tuning Controller (STC)

The structure of the STC is shown in Figure 2.2. An explicit separation of identification and control is assumed, in contrast to the MRAC, where the parameters of the controller are updated directly to achieve the goal of model following. The STC can be thought of as having two loops: an inner loop consisting of a conventional controller, but with varying parameters, and an outer loop consisting of an identifier and a design box which adjust controller parameters.

The STC is very flexible with respect to the choice of controller design

methodology (linear quadratic, deadbeat, pole placement, minimum variance and gain-phase margin design) and to the choice of identification scheme (least squares, extended and generalized least squares, instrumental variables, extended Kalman filtering and maximum likelihood). However, the analysis of self-tuning adaptive systems is more complex than that of model reference adaptive systems because the transformation from identifier parameters to controller parameters is usually non-linear (Astrom and Wittenmark, 1989).

Although the MRAC and the STC were introduced as different approaches, the principal difference between them is that the MRAC systems are direct adaptive schemes, whereas the STC approaches are indirect. The STC first identifies the plant parameters

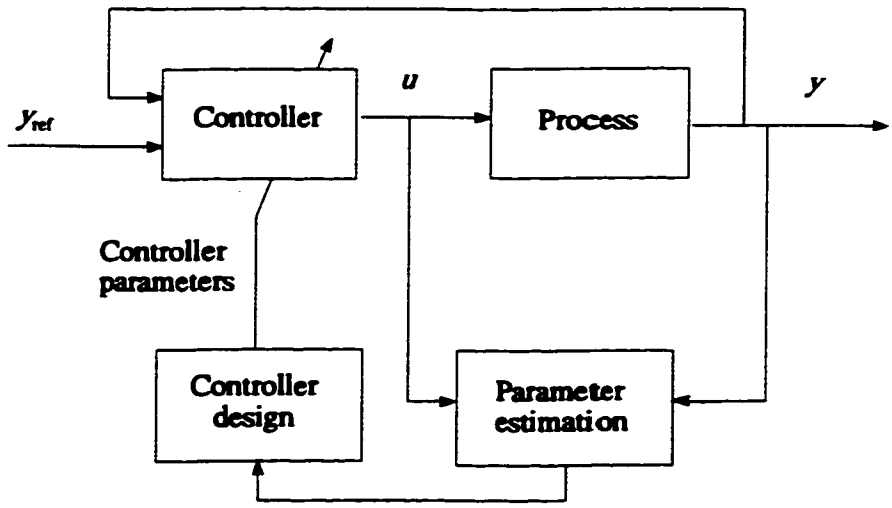

Figure 2.2 Block diagram of STC

recursively, and then uses these estimates to update the controller parameters through some fixed transformation. The MRAC schemes update the controller parameters directly. In other words, the MRAC can be seen as a special case of the STC, with an identity transformation between updated parameters and controller parameters. However, this difference is historic and not fundamental, because the STC can be modified so that the controller parameters are updated directly (Astrom and Wittenmark, 1989). Also researchers have developed various methods of indirect MRAC (Fussell, 1987).

2.2 Review of Adaptive Control in Machining Processes

2.2.1 Classification of Adaptive Control Systems

Adaptive control systems in machining processes can be classified into two categories (Koren, 1983; Ulsoy et al., 1983):

(1) Adaptive Control with Optimization (ACO), and

(2) Adaptive Control with Constraints (ACC).

ACO optimizes a performance index subject to process and system constraints. ACC attempts to hold a cutting process variable (cutting force, torque or power) constant by adjusting one or more process parameters.

Typically, feedrate or both the feedrate and spindle speed are manipulated in ACO to adjust cutting process. Although ACO may provide a more complete optimization of the machining process, it is very difficult to implement on a real system because of its complexities, both in defining and evaluating realistic performance indices and in measuring the necessary parameters on line reliably. ACO applications have been few

and limited mainly to grinding.

ACC systems, as opposed to ACO systems, are used extensively in milling, turning and drilling processes because of the ease of analysis and the low cost of implementation. The task of determining the index of performance has been eliminated along with the optimization routines. In most of the algorithms developed, cutting force is held constant by varying the feedrate (Ulsoy et al., 1983).

2.2.2 Development of Adaptive Control with Constraints (ACC) Systems

ACC systems may use either fixed gain or adaptive controllers. Those systems that use fixed gains, although termed "adaptive" in some manufacturing literature, are not adaptive systems as defined in the control literature (Ulsoy et al., 1983). Due to the inclusion of the cutting process in the control loop, variations in cutting process parameters may result in poor performance or even instability of the control system. Therefore, researchers have investigated various adaptive systems, from variable gain to MRAC and STC controllers in the last two decades.

Fixed and variable gain systems

Two typical fixed gain controllers were those of Milner (1975) and Tlusty et al. (1978). In Milner's work, a fixed gain Proportional-Integral (PI) control scheme was developed in which the end milling cutter deflection was measured and held to a constant reference value by feedrate adjustment. For the design of the controller and stability analysis, the transfer function of the end milling process was synthesized according to

the open-loop frequency response when driven by steady state sinusoidal input. Experimental results indicated that the controller worked satisfactorily only if the variations of the depth of cut were not too large. The PI controller developed by Tlusty et al (1978) was for force control in an end milling operation. The cutting force was measured by a table dynamometer. A first-order continuous model was used to represent the end milling process. To reduce the force load on the cutting tool during transient cutting, a two level adaptive control strategy was used in addition to the PI controller. It called for a very rapid deceleration of the feedrate when a sudden increase in depth of cut was detected.

Stute and Goetz (1976) proposed a variable gain PI controller for turning and milling processes. A fixed gain dynamic model parallel to the controlled process was used to assist the gain adjustment of the PI controller such that a constant open-loop gain specified by the parallel model was always maintained, despite variations in the controlled process gain. Koren and Masory (1981) implemented a variable gain ACC of cutting force in turning. They employed a simple on-line estimator for the process gain and an integral strategy to adjust the gain of an integral controller based on the estimated process gain.

These fixed and variable gain controllers have good performance only when process parameter variations are small. The gains used for tuning the controllers are determined by trial and error.

MRAC and STC systems

MRAC approaches have been successfully implemented in machining processes. The attractiveness of MRAC is due to the well-developed design method and convergence proofs. The standard MRAC scheme attempts to cancel the process poles and zeroes to provide perfect tracking.

Tomizuka, Oh and Dornfeld (1983) provided the first comprehensive investigation of parameter adaptive force control for an end milling machine. They applied a discrete-time MRAC algorithm based on the Independent Tracking and Regulation (ITR) technique (Landau and Lozano, 1981) to regulate the cutting force in an end milling operation. A first-order discrete-time model was used for the controller design. To eliminate the periodic force component caused by cutter runout, an average force per revolution was used to represent the cutting force level. In their experiments, oscillating transient behaviours were observed when both process time constant and gain were estimated. A better regulation performance was obtained by only estimating the process gain while fixing the pole of the cutting process at a constant value.

Lauderbaugh and Ulsoy (1988, 1989) developed a second-order empirical model based on feedrate input and instantaneous resultant force output, and used an MRAC controller based on the discrete-time MRAC technique of Goodwin and Sin (1984) to force control of an end milling process. Their simulation results indicated that the MRAC approach could yield a significantly better transient performance than the fixed gain PI controller and the controller was stable in the presence of large parameter variations. However, the controller did not perform well because of the biased estimates caused by

measurement noise due to cutter runout, which was not completely eliminated by the first-order digital low-pass filter they used.

Model reference adaptive control of cutting force in turning was considered by Daneshmend and Pak (1986) who used a first-order model to relate cutting force and feedrate. The MRAC technique of Landau and Lozano (1981) was implemented using an external nonadaptive loop and an integral controller. They compared several different algorithms derived from the MRAC design technique, and reported satisfactory results when only process gain was estimated. In the work of Fussell and Srivasan (1988), an outer fixed gain PI controller was added to the MRAC system and an algebraic scheme was used to reduce the force oscillations due to cutter runout. Their experimental results showed that the inclusion of the outer PI control loop in the scheme could bring the cutting force to the desired level more rapidly than those using MRAC scheme alone. But there was no improvement in the magnitude of the transient force peaks occurring during the abrupt change in the geometry of cut.

The application of the STC was investigated by Elbastawi and Sagherian (1987) for force control of end milling process. They examined several STC strategies such as deadbeat (DB), deadbeat with increased order (DB2), discrete Proportional-Integral-Derivative (PID) and pole placement control. The strategies were shown to be stable and have good performance characteristics. A better performance was observed using the DB2 and discrete PID controllers in terms of the transients of a step change in the axial depth of cut. A pole placement STC applied to the force control of the end milling process was discussed by Altintas (1994). The adaptive controller was designed in such

a way that its closed loop characteristic function behaved like an open loop regular and stable machining operation. Their simulation and experimental results justified the viability of the method.

Most of the above control schemes are designed for non-minimum phase systems. Consequently, they can only be applied to systems with very stable zeros.

Adaptive control systems for non-minimum phase end milling processes

In control systems, the plant time delay and excess continuous-time poles can lead to discrete-time non-minimum phase zeros (Astrom et al., 1984). In machining process control, calculation and implementation of control command, construction and filtering of output signals, etc., can all cause process time delay. Therefore a non-minimum phase operation is very likely to exist in end milling processes (Liu and Liang, 1989). To address this problem, Liu and Liang (1989) proposed a modified MRAC approach based on the quasi-direct adaptive controller of Lozano and Landau (1982). This approach was in fact a combination of the MRAC structure and the indirect STC in which the controller was designed by a pole-placement approach. Liu and Liang (1989) showed the controller's feasibility for force control of end milling process through simulation in a deterministic environment using Lauderbaugh and Ulsoy's (1989) second-order process model. The modified MRAC is a typical one among the adaptive controllers developed for non-minimum phase end milling processes during the last few years. It is comparatively complex to design and implement and is sensitive to process parameter variations, as shown later in this thesis.

Kolarits and DeVries (1990) presented the experimental evaluation of Liu and Liang's (1989) modified MRAC controller to the force control of end milling processes. High transient peaks and oscillating feedrate input were observed in force control of the end milling process which had a feed drive with slow response. Barthel and Shin (1993) developed a modified quasi-direct MRAC algorithm based on the quasi-direct adaptive controller of Lozano and Landau (1982) and gave simulation results for force control of end milling processes. The principal modification was the incorporation of a zero phase error tracking controller to compensate for the phase and gain of the process zero without pure cancellation of zeros in the numerator.

Kim and Huang (1992) used a first-order discrete model to represent an end milling system and applied a pole-placement STC to the force adaptive control of the process. The design methodology of the controller is similar to that of Liu and Liang's (1989) modified MRAC approach. The end milling process they considered was a non-minimum phase system in which the computational delay exceeds one half of the control interval. Satisfactory experimental results were reported.

The above adaptive controllers were investigated on end milling processes which had a time delay not exceeding the sampling interval. They are indirect adaptive schemes and hence are only suitable for non-minimum phase end milling systems with a low order model.

Chapter 3

Modelling and Identification of the End Milling Process

The availability of an appropriate dynamic model is essential to the design and evaluation of adaptive control systems. The model should be able to predict accurately the steady-state and transient process outputs for a wide range of cutting conditions. In this chapter, the dynamic model relating the command feedrate and the spindle power or cutting force of the end milling process will be developed. Using open-loop cutting tests, the adequacy of the developed model will be validated and parameters for the power and force systems will be identified for a variety of cutting conditions.

3.1 Experimental Set-Up

The experimental set-up of the end milling system for spindle power and cutting force control is presented in the following sections. The technical data and configuration of the experimental equipments (power sensor, force sensor and charge amplifiers) are given in Appendix A.

3.1.1 Milling Machine and Cutting Conditions

The vertical CNC (Computer Numerically Controlled) milling machine (Servo 2000) built by the Servo Products Co. was used. The spindle motor is a three-phase AC induction motor which is driven by a G3, 3 HP AC motor drive. The motor output power is transmitted by a set of pulleys and transmission belts to the spindle shaft hub. In high gear, the clutch is engaged, connecting the power from the spindle shaft hub to the spindle shaft directly. In low gear, the clutch is disconnected and the power from the spindle shaft hub goes through a set of pulleys and gears to the spindle shaft. The spindle speed in high gear ranges from 450 to 5100 rpm, while in low gear, the speed can vary

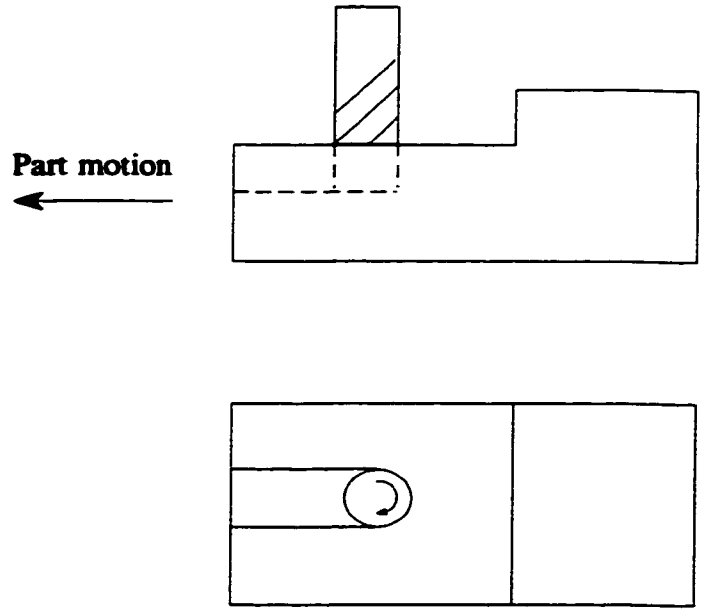

Figure 3.1 Schematic of slot-milling

from 45 to 510 rpm. The machine has three sliding axes, with the *X* (table) and *Y* (cross) axes driven by axis drive motors and lead screws. The axis drive motors are 3-phase Variable Reluctance stepping motors with a resolution of 84 primary steps per revolution.

High Speed Steel (HSS) 14.3 mm end milling cutters with four helical flutes and 30° helix angles were used. The spindle speed was 300 rpm. Slot milling, or full-immersion milling (as illustrated in Figure 3.1) without coolant along *Y*-axis was performed on C1018 cold rolled steel workpieces.

3.1.2 Measurement and Preprocessing of Power Signals

The experimental set-up of the power control system is shown in Figure 3.2. The power sensor (Load Controls PH-3A) was mounted by passing the three input electrical cables of the motor through the cell. The power sensor had a full scale power capacity of 5 HP and a voltage output ranging from 0 to 10 Volts, leading to a sensitivity of 2 V/HP. The spindle power signals measured by the power sensor were band-limited by a 4th-order Butterworth low-pass filter with cut-off frequency of 2 Hz to eliminate noise due to cutter runout, belt oscillation and spindle motor speed (Fussell, 1987; Stein and Wang, 1990). The filtered power signals were then digitalized by a 12 bit A/D converter.

3.1.3 Measurement and Preprocessing of Force Signals

Figure 3.3 shows the experimental set-up of the force control system. The dynamometer was mounted on the table of the milling machine between two steel plates.

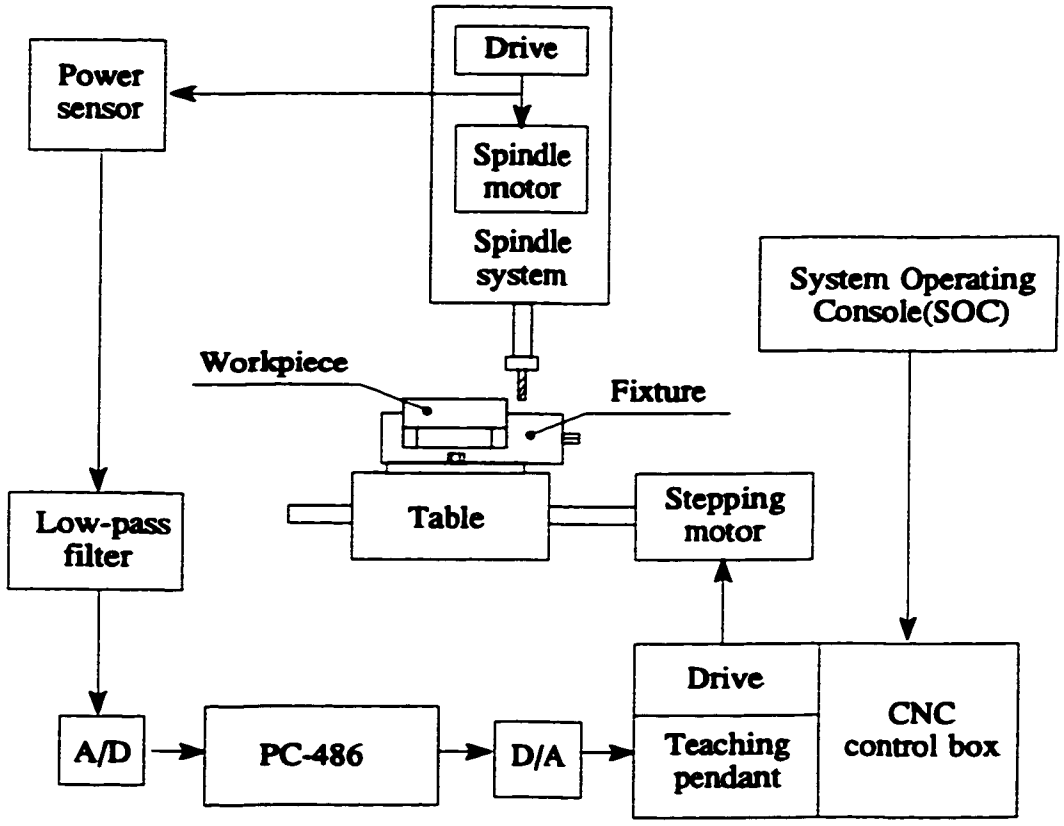

Figure 3.2 Experimental set-up of the spindle power control system

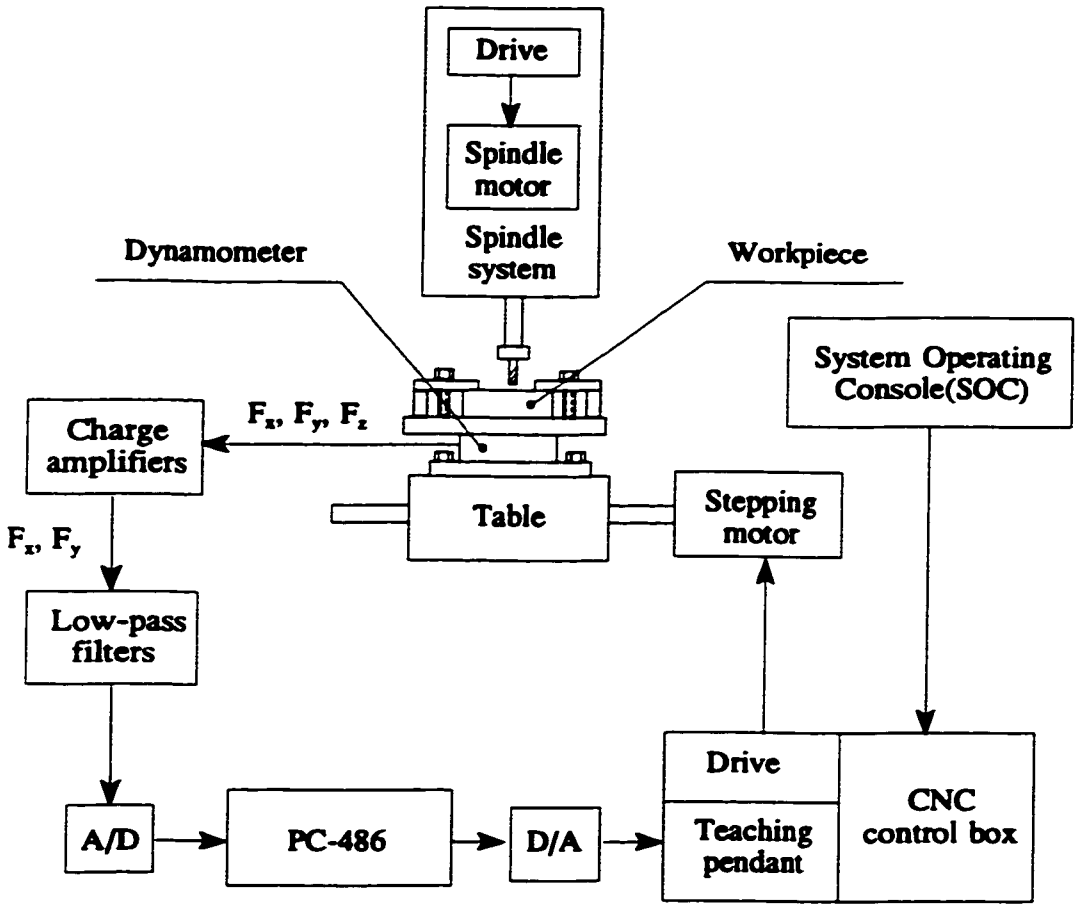

Figure 3.3 Experimental set-up of the cutting force control system

The workpiece was mounted on the top of the upper steel plate. The X and Y axis components of the cutting force measured by the dynamometer were amplified by charge amplifiers with a sensitivity of 0.002 V/N, and then passed through 4-th order Butterworth low-pass filters with cut-off frequency of 2 Hz to eliminate noise due to cutter runout (Fussell, 1987). The filtered force signals were then digitalized by a 12 bit A/D converter. The resultant cutting force F_c acting on the cutter was reconstructed by implementing:

$$F_c = (F_x^2 + F_y^2)^{1/2} \tag{3.1}$$

where F_x and F_y are the X (table) and Y (cross) cutting force components which lie in the plane of the machine tool table.

3.1.4 Feedrate Command Implementation

The mill was modified at the feedrate overriding circuit of the control box so that the feedrate overriding by the controlling computer could be implemented. The command feedrate in a form of overriding percentage of the full scale feedrate was converted to an analog voltage signal ranging from 0 to 5 V by the 12 bit D/A converter and then sent to the feedrate overriding circuit. The full scale (100%) feedrate was set at the System Operating Console (SOC) of the milling machine tool. The feedrate could be changed from 0 to 150 percent of the full scale feedrate.

3.2 End Milling Process Model

Figure 3.4 shows the block diagram of the end milling system. The system

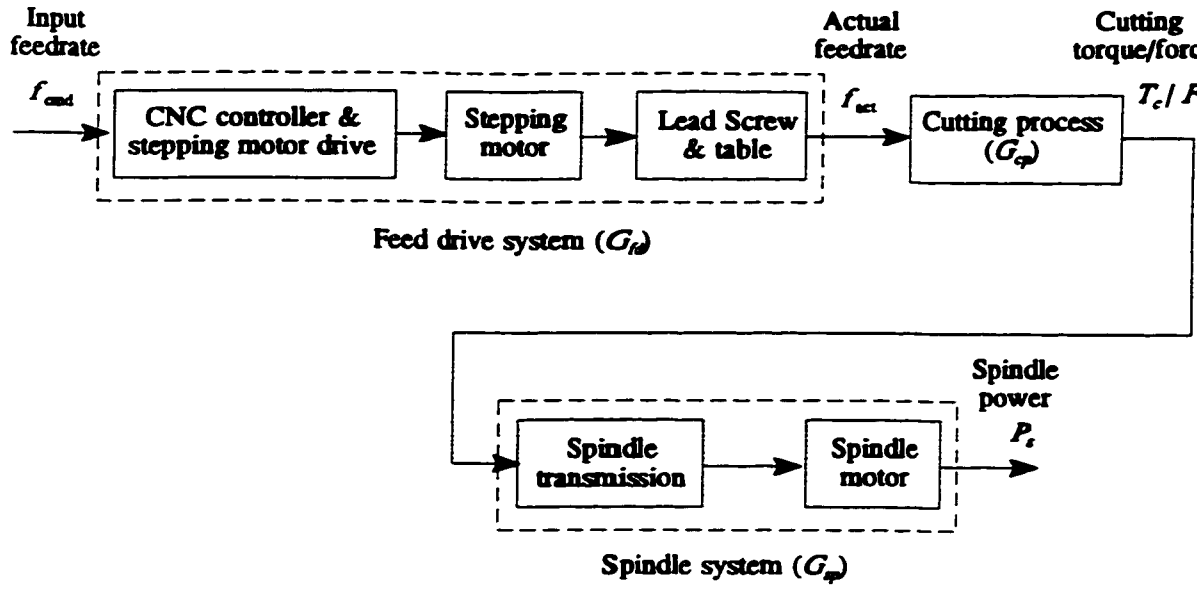

Figure 3.4 Block diagram of the end milling process

consists of three subsystems: the feed drive system G_{fd}, the cutting process G_{cp}, and the spindle system G_{sp}. The feed drive system and spindle system are treated as time-invariant and the dynamics of the cutting process as time-varying.

3.2.1 Cutting Process Model

Modelling of the end milling process has been studied by many researchers and much of the work has been intended for detailed mechanistic analysis of the steady-state end milling process (Kolarits and DeVries, 1991; Smith and Tlusty, 1991; Tlusty and MacNeil, 1975). After consideration of the parameters such as the cutter deflection, the time-varying forces and the tooth helix position, the models turned out to be either high order, nonlinear, or iterative types. For controller design, researchers such as Tomizuka

et al. (1983), Hsu and Hsieh (1994) and Altintas (1994) have performed analyses and obtained first or second-order linear models. In this research, a first-order model is adopted to represent the dynamics between the actual feedrate f_{act} and the resulting cutting torque T_c (Tomizuka, 1983; Kim and Huang, 1992):

$$G_{cp}(s) = \frac{T_c(s)}{f_{act}(s)} = \frac{K_{cp}}{1 + \tau_{cp} s} \tag{3.2}$$

where $G_{cp}(s)$ is the transfer function of the cutting process, K_{cp} the cutting process gain, τ_{cp} the cutting process time constant and s the LaPlace transform operator. Both K_{cp} and τ_{cp} are treated as time-variant.

F_c and T_c are linearly related by:

$$\frac{F_c(s)}{T_c(s)} = K_{ft} \tag{3.3}$$

where K_{ft} is the force-to-torque gain.

3.2.2 Feed Drive System and Spindle System Models

The table axes are driven by stepping motors and their transient behaviours are generally three times or more faster than that of the cutting process dynamics (Lauderbaugh and Ulsoy, 1988; Kolarits and DeVries, 1991). Consequently, the dynamics of the feed drive system, which includes the CNC controller, stepping motors and their drives, lead screws and table, can be treated as a constant gain:

$$G_{fd}(s) = \frac{f_{act}(s)}{f_{cmd}(s)} = K_{fd} \tag{3.4}$$

where $G_{fd}(s)$ is the transfer function of the feed drive system, $f_{cmd}(s)$ the command feedrate, $f_{act}(s)$ the actual feedrate, and K_{fd} the gain of the feed drive system.

In the spindle system, the mechanical power carried by motor shaft is transferred to spindle shaft through a system of pulleys with a belt, and a clutch (in high gear) or a gear set (in low gear). Stein and Wang (1990) have analysed the power monitoring of AC inductive motors in spindle systems for sensing cutting torque. Their results showed that the transient characteristics of the spindle system could be approximated by a linear second-order system. The bandwidth of the spindle system was approximately 18 Hz at 600 rpm and 12 Hz at 1504 rpm.

The torque on the motor shaft T_e can be determined by:

$$T_e = \frac{P_g}{\omega_s} \tag{3.5}$$

where ω_s is the synchronous speed of motor and P_g the rotor input power which is the difference between the electrical input power (i.e., spindle power) P_s and the power losses in the stator windings. Under constant spindle speed, the relationship between T_e and P_g can be considered to be static.

The static relation between the cutting torque and the spindle motor torque is (Stein and Wang, 1990):

$$T_e = n_s T_c + T_f + B_v \omega_m \tag{3.6}$$

where T_f is the Coulomb friction, B_v the viscous damping coefficient, ω_m the angular speed of motor and n_s the spindle-to-motor speed ratio.

The Coulomb friction and viscous damping torques do not vary with cutting

torque (Stein and Wang, 1990). Thus changes in motor torque, ΔT_e, are proportional to changes in the cutting torque ΔT_c. The static sensitivity of the spindle system then is:

$$\frac{\Delta P_g}{\Delta T_c} = n_s \omega_s \tag{3.7}$$

where ΔP_g refers to the change in rotor input power.

In typical cutting conditions, the power loss due to the stator windings is a small constant (Stein and Wang, 1990). Therefore, at low and constant spindle speeds, the spindle system dynamics can be modelled as a gain, that is:

$$G_{sp}(s) = \frac{P_s(s)}{T_c(s)} = K_{sp} \tag{3.8}$$

where $G_{sp}(s)$ is the transfer function of the spindle system and K_{sp} is the gain of the spindle system.

3.2.3 End Milling Process Model and its Discrete-time Equivalence

The above discussions show that the machining process is reduced to a simplified system as shown in Figure 3.5. Consequently, the dynamics of spindle power and cutting force systems are:

$$\frac{P_s(s)}{f_{cmd}(s)} = G_{fd}(s) \cdot G_{cp}(s) \cdot G_{sp}(s) = K_{fd} \cdot G_{cp}(s) \cdot K_{sp} = \frac{K_{fd} K_{cp} K_{sp}}{1 + \tau_{cp} s} \tag{3.9}$$

$$\frac{F_c(s)}{f_{cmd}(s)} = G_{fd}(s) \cdot G_{cp}(s) \cdot \frac{F_c}{T_c} = K_{fd} \cdot G_{cp}(s) \cdot K_{ft} = \frac{K_{fd} K_{cp} K_{ft}}{1 + \tau_{cp} s} \tag{3.10}$$

Therefore the end milling process can be modelled as a first-order system with time-varying parameters for both spindle power and cutting force systems:

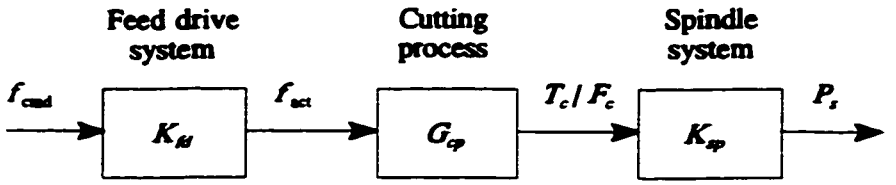

Figure 3.5 Simplified block diagram of the end milling process

$$G_p(s) = \frac{K}{1+\tau s} \tag{3.11}$$

where $G_p(s)$ is the transfer function of the end milling process, K is the system gain and τ the system time constant.

In general, there is a process time delay caused by signal construction, control computation and feedrate command implementation. As a result, the transfer function Equation (3.11) can be extended to the following form to include the delay time:

$$G_p(s) = \frac{K}{1+\tau s} e^{-\delta s} \tag{3.12}$$

where δ is the delay time which has the following form (Franklin et al., 1990):

$$\delta = dT - mT \tag{3.13}$$

where d is the time delay step which is an integer, m is the fractional delay step which is a number less than one. T is the control interval.

The resulting zero-order-hold equivalent discrete time end milling process is (see

Appendix B for derivation):

$$G_p(z) = z^{-d}\frac{b_0 + b_1 z^{-1}}{1 + a_1 z^{-1}} \tag{3.14}$$

with

$$a_1 = -e^{-T/\tau} \tag{3.15}$$

$$b_0 = K(1 - e^{-mT/\tau}) \tag{3.16}$$

$$b_1 = K(e^{-mT/\tau} - e^{-T/\tau}) \tag{3.17}$$

and z^{-1} is the backward-shift operator.

The system has one pole, one zero and a time delay of d steps. The zero is at

$$-\frac{b_1}{b_0} = -\frac{e^{-mT/\tau} - e^{-T/\tau}}{1 - e^{-mT/\tau}} \tag{3.18}$$

and it varies with T, τ and m. At certain T and τ, it moves toward the center of the unit circle as $m \to 1$ and moves outside as $m \to 0$. Therefore depending on the value of time delay, the process can be a minimum phase or non-minimum phase system.

3.3 Model Verification and Process Parameter Identification Using Open-Loop Experiments

The step-response method was utilized for verifying the established model and identifying process parameters of the end milling process. The parameter a_1 at different depths of cut was identified by fitting the end milling process model Equation (3.14) to the corresponding step-response samples using the Recursive Least Square (RLS) off-line identification technique (Ljung, 1987). Process gains K for different depths of cut at

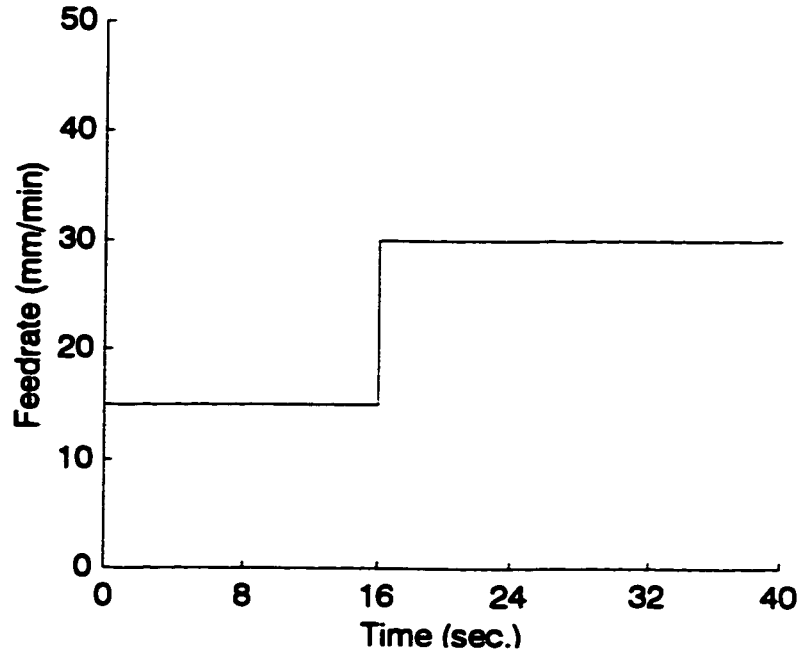

Figure 3.6 Step change of feedrate for process identification

different feedrates were calculated from the feedrate input and the average power or force output.

The listing of the m-file for process parameter identification is given in Appendix C.

Slot milling was performed on C1018 cold rolled steel using a four-tooth 14.3 mm HSS helical cutter. The spindle speed was set at 300 rpm. The experiments were repeated at three different depths: 1.78 mm, 2.79 mm and 3.81 mm. The rate of signal sampling was 5 Hz, the same as the spindle frequency. Hence the sampling interval was 0.2 seconds. To estimate a_1, a step change of feedrate from 15 mm/min to 30 mm/min was

used, as shown in Figure 3.6. To evaluate K, the spindle power and the cutting force at feedrates of 15, 22.5 and 30 mm/min were sampled. The average power $\overline{P}_s$ and average force $\overline{F}_c$ for these feedrates were then calculated.

3.3.1 Spindle Power System

Examining the step responses of the power signal indicates that the spindle power system has the characteristics of a first-order process for all three depths of cut, which justifies the modelling methodology of Section 3.2. Figure 3.7 presents the power samples for 1.78 mm depth of cut, with Figure 3.7(a) showing the full samples and Figure 3.7(b) giving the samples during the feedrate change. The time delay of the filtered power signal was found to be about 0.3 to 0.4 seconds. With the delay

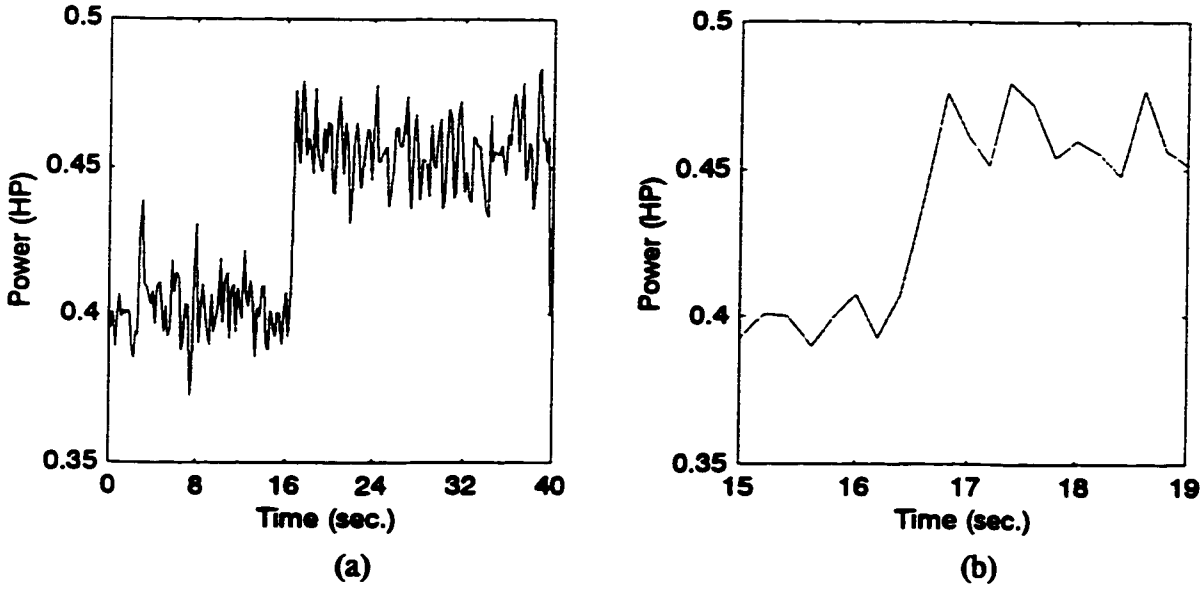

Figure 3.7 Spindle power signal sampled at 1.78 mm depth of cut
(a) the full samples (b) the samples during the feedrate change

parameter of the off-line RLS estimation scheme set to 2, the values of parameter a_1 were estimated as listed in Table 3.1. Results of average spindle power levels for three feedrates at different depths of cut, and the gains calculated thereafter are shown in Table 3.2.

Depth of cut, a (mm)	1.78	2.79	3.81
a_1	−0.66	−0.74	−0.80

Table 3.1 Parameter a_1 under different depths of cut a for the spindle power system

Depth of cut, a (mm)		1.78	2.79	3.81
$\overline{P}_s$ (HP)	low	0.393	0.417	0.458
	medium	0.400	0.450	0.522
	high	0.449	0.479	0.560
K (HP/mmpm)	low	0.026	0.028	0.031
	medium	0.019	0.020	0.023
	high	0.015	0.016	0.019

* Low, medium and high refer to feedrates of 15, 22.5 and 30 mm/min respectively

Table 3.2 Average power $\overline{P}_s$ and system gain K at different feedrates with different depths of cut a for the spindle power system

To observe how the model parameters vary with depth of cut and feedrate, the parameter a_1 under different depths of cut is plotted in Figure 3.8(a). In the figure, a_1 appears to be decreasing nonlinearly with depths of cut. In Figure 3.8(b), parameter K for different feedrates at different depths of cut is plotted. It is observed that K decreases nonlinearly with feedrate and increases as the depth of cut increases.

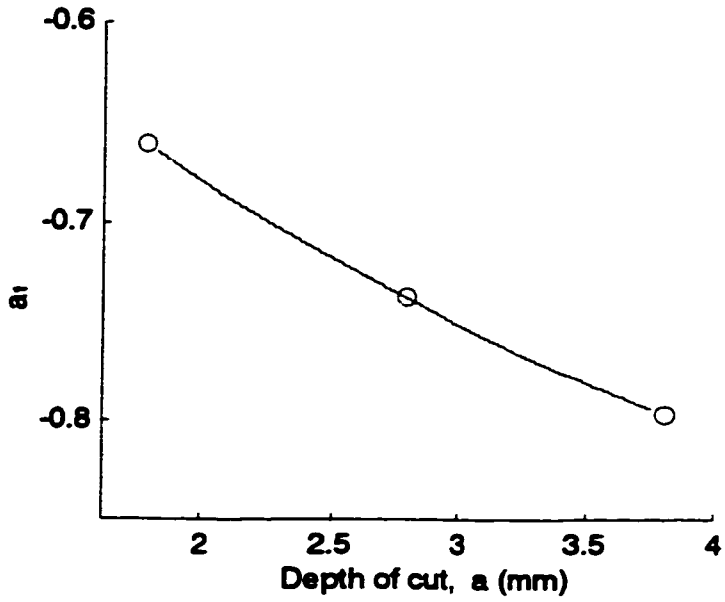

(a)

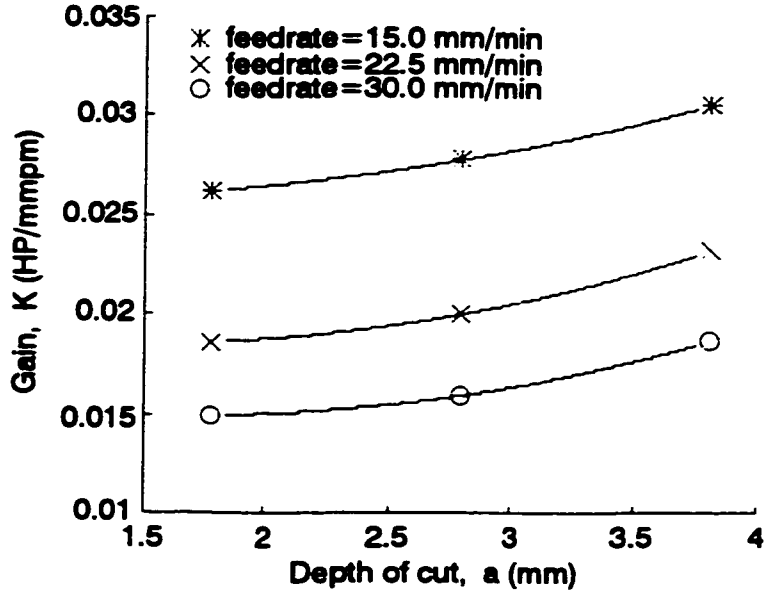

(b)

Figure 3.8 Process parameters a_1 and K versus depth of cut a for the spindle power system

3.3.2 Cutting Force System

Samples of the cutting force step-response tests also showed the characteristics of a first-order plant for all three depths of cut. The force samples for 1.78 mm depth of cut are given in Figure 3.9, with Figure 3.9(a) and (b) showing the full samples and the samples during the feedrate change respectively. The process time delay was evaluated as about 0.5 to 0.6 seconds. The values of a_1 obtained through estimation with the delay parameter of the off-line RLS estimation scheme set to 3 are listed in Table 3.3. The values of average force for different feedrates and different depths of cut, and the gains thus calculated are listed in Table 3.4.

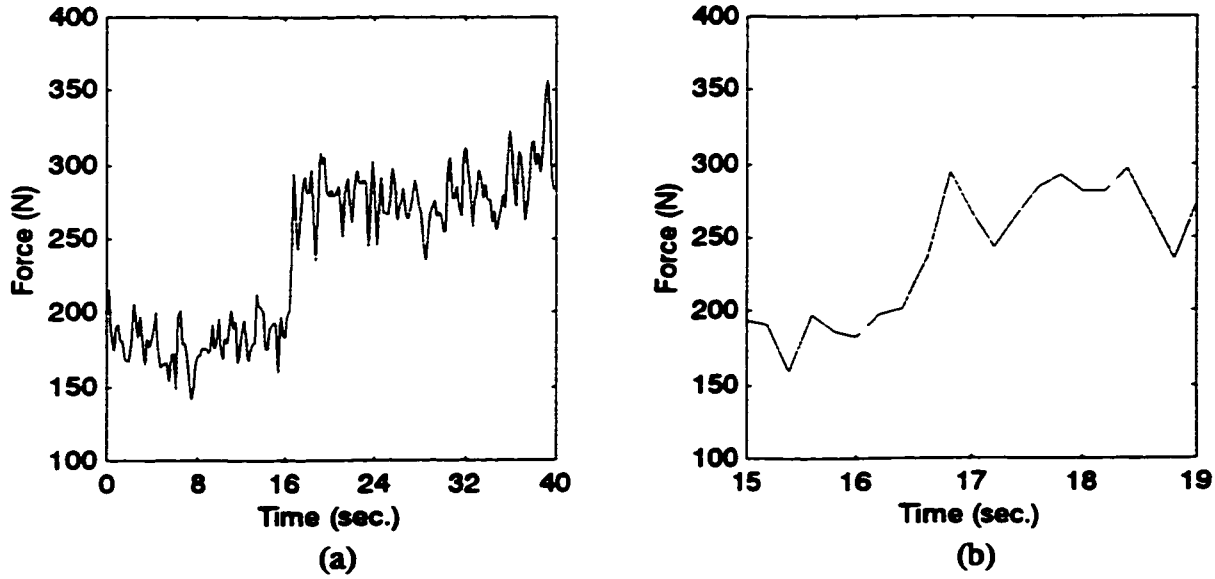

Figure 3.9 Cutting force signals sampled at 1.78 mm depth of cut
(a) the full samples (b) the samples during the feedrate change

The results are plotted in Figure 3.10(a) and 3.10(b). Again, a_1 decreases nonlinearly with depth of cut. K increases nonlinearly with depth of cut and decreases with feedrate.

Depth of cut, a (mm)	1.78	2.79	3.81
a_1	−0.60	−0.78	−0.82

Table 3.3 Parameter a_1 under different depths of cut a for the cutting force system

Depth of cut, a (mm)		1.78	2.79	3.81
$\overline{F}_c$ (N)	low	133.7	198.2	279.3
	medium	184.4	289.0	393.5
	high	233.9	351.3	516.3
K (N/mmpm)	low	8.9	13.2	18.6
	medium	8.2	12.8	17.5
	high	7.8	11.7	17.2

* Low, medium and high refer to feedrates of 15, 22.5 and 30 mm/min respectively

Table 3.4 Average force $\overline{F}_c$ and system gain K at different feedrates with different depths of cut a for the cutting force system

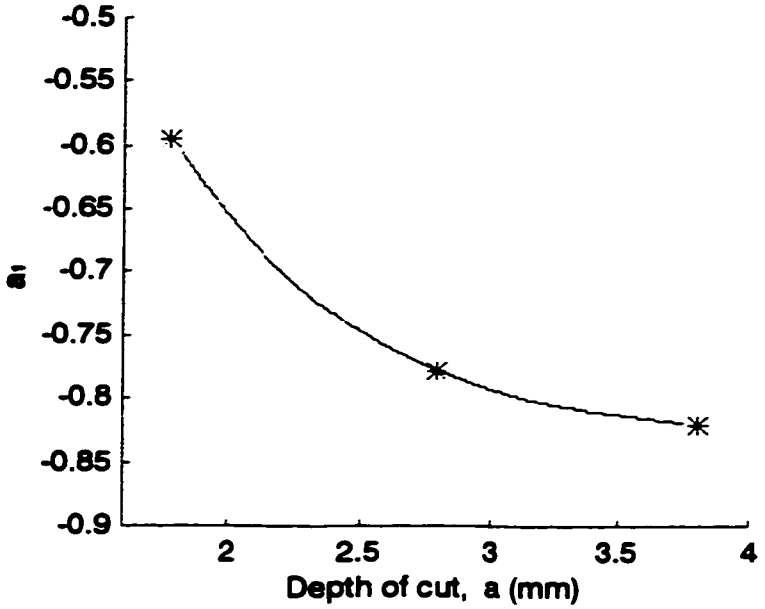

(a)

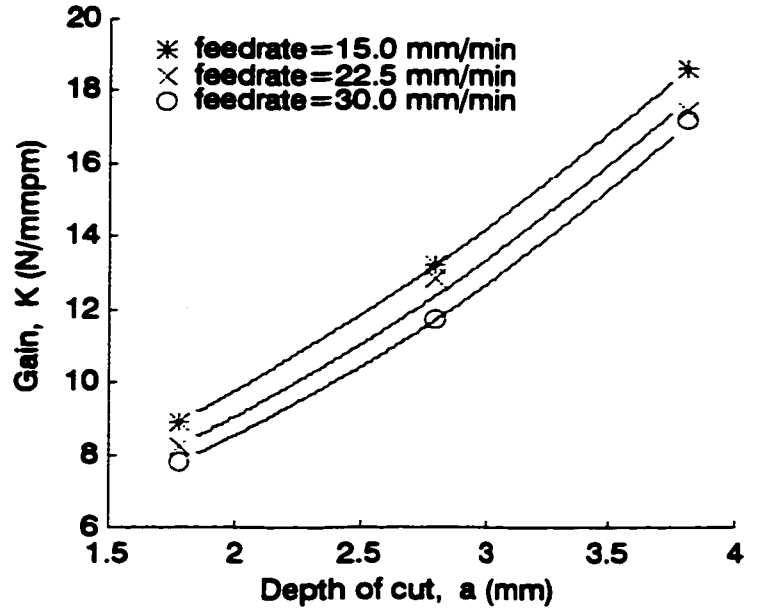

(b)

Figure 3.10 Process parameters a_1 and K versus depth of cut a for the cutting force system

Chapter 4

Design and Evaluation of Adaptive Controllers

In Chapter 3, the milling system has been modelled as a linear time-varying first-order plant with one pole, one zero and pure time delay. The zero of the process can be outside of the unit disk, thus leading to a non-minimum phase process. As demonstrated by Liu and Liang (1989), conventional discrete MRAC's based on cancellation of the process zeros by the controller's poles may result in an unstable control system in controlling non-minimum phase processes. In this thesis, two adaptive control schemes capable of dealing with non-minimum phase end milling processes are examined. One is DB MRAC (Butler, 1992). The other is Liu and Liang's (1989) modified MRAC, which is a typical algorithm developed for non-minimum phase end milling processes in recent years. Both control algorithms are based on indirect, or explicit methods. The commonly used RLS parameter estimation algorithm is used to identify the time-varying milling process parameters on-line.

In this chapter, Section 4.1 describes the RLS estimation algorithm. The model parameters used in controller simulations are given in Section 4.2. The design of the DB

MRAC and the modified DB MRAC, as well as the evaluation of these two adaptive control algorithms by simulations are presented in Section 4.3.

4.1 On-Line Parameter Estimation Algorithm

In this research, the design of adaptive controllers is based on the indirect, or explicit method, which means that the design of the control law is developed by treating the estimated process parameters as if they were true process parameters (Goodwin and Sin, 1984). The RLS parameter estimation algorithm is used to estimate them in real time.

The transfer function of the cutting process shown in Equation (3.14) can be expressed in the following linear recursive form:

$$A(z^{-1})y(k) = z^{-d}B(z^{-1})u(k) \tag{4.1}$$

with $A(z^{-1}) = 1 + a_1 z^{-1}$

$B(z^{-1}) = b_0 + b_1 z^{-1}$

where d is the time delay. It can be written in an alternative form as:

$$y(k) = -a_1 y(k-1) + b_0 u(k-d) + b_1 u(k-d-1) \tag{4.2}$$

The regression model is then:

$$y(k) = \phi^T(k-d)\,\theta\,(k-1) \tag{4.3}$$

with $\phi(k-d) = [y(k-1),\ u(k-d),\ u(k-d-1)]^T$

$\theta(k-1) = [-a_1,\ b_0,\ b_1]^T$

where θ is the parameter vector, ϕ is the input and output vector. The initial parameter vector θ (0) was set to [0.5, 0.01, 0.01].

The estimation of the parameters $\theta(k)$ is recursively updated as follows (Goodwin and Sin, 1984; Kolarits and DeVries, 1990):

$$\theta(k) = \theta(k-1) + P(k)\phi(k-1)\varepsilon(k); \quad k \geq 1 \tag{4.4}$$

with

$$\varepsilon(k) = \frac{y(k) - \theta^T(k-1)\phi(k-1)}{\lambda(k) + \phi(k-1)^T P(k)\phi(k-1)} \tag{4.5}$$

The covariance matrix $P(k)$ is updated as the following:

$$P(k+1) = \frac{1}{\lambda(k)}\left[P(k) - \frac{P(k)\phi(k-d)\phi^T(k-d)P(k)}{\lambda(k) + \phi^T(k-d)P(k)\phi(k-d)}\right] \tag{4.6}$$

where ε is the tracking error and λ is the forgetting factor. For the milling process (Equation (3.14)), P is a 3×3 matrix.

Some modifications which make the RLS algorithm more applicable to time-varying systems were used. One technique was to reset the covariance matrix P to the initial value when the trace of the P matrix was less than a threshold value, i.e.:

$$P(k) = \alpha I \tag{4.7}$$

where I is the identity matrix and α is the covariance matrix resetting factor which is a positive scalar. By resetting the covariance matrix, the estimator is maintained at a fast convergence rate and kept alert to parameter variations. In the simulation studies presented in Section 4.3 and 4.4, the value of α was chosen to be 1000. In the experiments to be discussed in Chapter 5, the value of α was set to 500 and 1000 for spindle power and cutting force adaptive control respectively. The selection of these values was done by trial and error.

Exponential data weighting, which has been frequently used in time-varying

system parameter estimation by attaching greater weighting to more recent data, was also employed. As Goodwin and Sin (1984) suggested, $\lambda(k)$ was chosen to be:

$$\lambda(k) = \lambda_0 \lambda(k-1) + (1-\lambda_0) \tag{4.8}$$

with $\lambda(0)=0.95$, $\lambda_0=0.99$, where λ_0 is the factor for discarding initial data.

In order to make the algorithm responsive to sudden changes in process parameters, $\lambda(k)$ was reset to $\lambda(0)$ when the tracking error $\varepsilon(k)$ was greater than a threshold value. By trial and error, this threshold was set to 0.03 in later simulations and experiments.

When the trace of the covariance matrix P was less than the lower trace limit, $\lambda(k)$ was reset to the initial value. In addition, to prevent the elements in the P matrix from becoming too large during steady-state operations due to the lack of system dynamic information, $\lambda(k)$ was set to 1 if the trace of P matrix was larger than a threshold (Fortescue et al., 1981).

By trial and error in the later simulations and experiments, the lower and upper limits of the trace of P matrix were set to $\alpha/5$ and 5α respectively.

4.2 Simulated Cutting Conditions

For the design and simulation of the adaptive controllers, the variation of cutting conditions was assumed to be the step changes in the depth of cut (1.78, 2.79 and 3.81 mm), as shown in Figure 4.1. The desired constant power and force levels were set at moderate values of 0.4 HP and 330 N respectively. These values were chosen so that the overall system behaved as a linear system. Considering that the maximum feedrate in real

cutting should be limited for prevention of tool damage, the maximum feedrate command was set at 100 mm/min.

For adaptive control of end milling processes, sampling intervals ranging from 0.03 to 0.125 seconds have been used by researchers (Fussell and Srinivasan, 1988; Tomizuka et al., 1983; Kim and Huang, 1992; etc.). Considering the long time delay of the power and force systems in the end milling process, the sampling interval was chosen to be 0.2 seconds in the simulation studies of the adaptive control algorithms. From Section 3.3, the time delays of the power and force systems were estimated to be about 0.3 to 0.4 and 0.5 to 0.6 seconds respectively, being approximately 2 and 3 times of the sampling interval. Hence the power system has a two-point delay (d=2) model and the force system has a three-point (d=3) model.

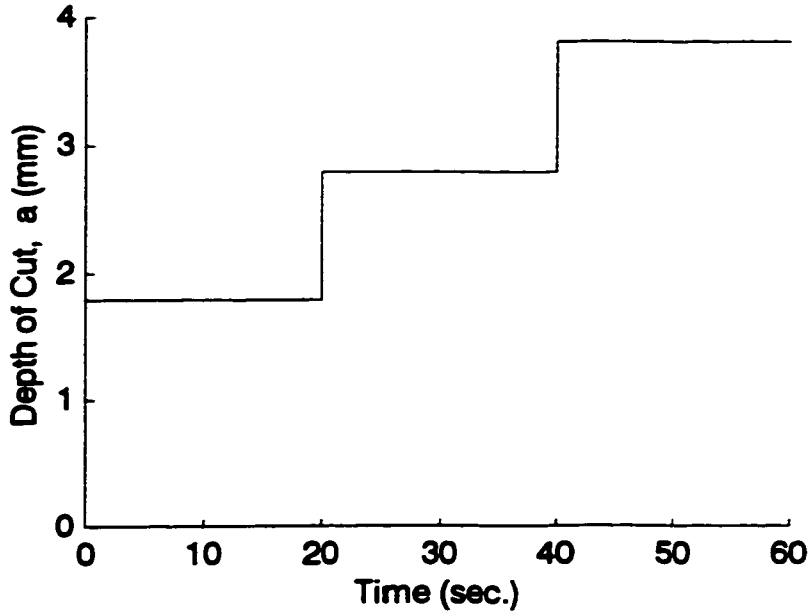

Figure 4.1 Depth of cut variation for control simulation

The fractional delay step was assumed to be 0.3, leading to non-minimum phase power and force systems in which the zeros are outside the unit circle (Equation (3.18)).

The values of a_1 under different depths of cut for the spindle power and cutting force systems were given in Table 3.1 and 3.3. It was shown in the Section 3.3 that the parameter K varied with feedrate and depth of cut. For a certain depth of cut, the lower the feedrate, the higher the value of K. By examining the curves of power and force system gains plotted in Figure 3.8(b) and referring to the feedrates used for different depths of cut in simulated controls, the values of K were assumed to be 0.012, 0.02 and

Depth of cut a (mm)	a_1	K (HP/mmpm)	b_0	b_1	$-b_1/b_0$
1.78	−0.66	0.012	0.00141	0.00267	-1.894
2.79	−0.74	0.020	0.00173	0.00347	-2.006
3.81	−0.80	0.030	0.00194	0.00406	-2.093

Table 4.1 Parameters of the discrete end milling process model under three different depths of cut for control simulation of the spindle power system

Depth of cut a (mm)	a_1	K (N/mmpm)	b_0	b_1	$-b_1/b_0$
1.78	−0.60	8	1.137	2.063	-1.814
2.79	−0.78	12	0.862	1.778	-2.063
3.81	−0.82	19	1.098	2.322	-2.115

Table 4.2 Parameters of the discrete end milling process model under three different depths of cut for control simulation of the cutting force system

0.03 for the three depths of cut in the spindle power system. Similarly, referring to Figure 3.10(b), the values of K under the three different depths of cut were assumed to be 8, 12 and 19 for the cutting force system. The values of b_0, b_1 and process zero $-b_1/b_0$ were then calculated from Equations (3.15) to (3.18). The parameters thus obtained for the spindle power and cutting force systems are summarized in Table 4.1 and 4.2

4.3 DB MRAC Scheme

4.3.1 DB MRAC Design

DB MRAC is an MRAC scheme making use of a "ripple-free" control strategy (Butler, 1992). It has a ripple-free or minimum-variance response, i.e., the system input and output responses reach their respective steady-state values in a finite settling time. Therefore the plant response will ideally track the reference input signal with zero tracking error after a finite time and for all time thereafter. The structure of the DB MRAC is shown in Figure 4.2.

For the plant G_p defined by:

$$\frac{y(k)}{u(k)} = \frac{z^{-d}B(z^{-1})}{A(z^{-1})} \tag{4.9}$$

with $A(z^{-1}) = 1+a_1z^{-1}+a_2z^{-2}+\cdots+a_{n_a}z^{-n_a}$

$B(z^{-1}) = b_0+b_1z^{-1}+b_2z^{-2}+\cdots+b_{n_b}z^{-n_b}$

where $\{y(k)\}$ and $\{u(k)\}$ are the plant output (spindle power or cutting force) and input (feedrate) sequences respectively, d the time delay, n_a and n_b the orders of $A(z^{-1})$ and $B(z^{-1})$

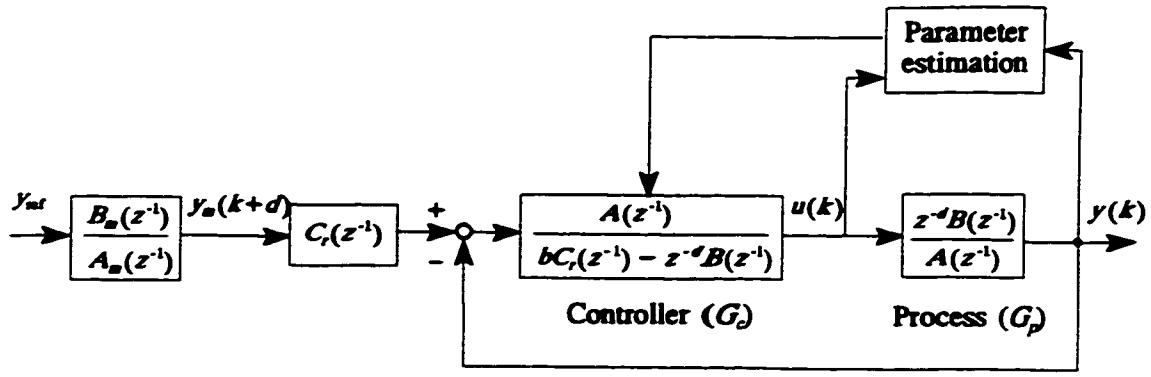

Figure 4.2 Structure of DB MRAC

respectively. The desired system tracking is given by the following reference model:

$$\frac{y_m(k)}{y_{ref}(k)} = \frac{z^{-d}B_m(z^{-1})}{A_m(z^{-1})} \tag{4.10}$$

where $y_m(k)$ is the output of the reference model and $y_{ref}(k)$ is the reference input.

In this thesis, the desired power or force level y_{ref} is a constant value, thus $A_m(z^{-1})$ and $B_m(z^{-1})$ are both selected to be 1. This yields:

$$y_m(k+d) = y_{ref} \tag{4.11}$$

The transfer function of the DB MRAC controller is:

$$G_c(z) = \frac{A(z^{-1})}{bC_r(z^{-1}) - z^{-d}B(z^{-1})} \tag{4.12}$$

with $b = \sum_{i=0}^{n_b} b_i$

$C_r(z^{-1}) = 1 + c_1 z^{-1} + c_2 z^{-2} + \cdots$

where the parameter b is a compensation for the DC gain of $B(z^{-1})$ and $C_r(z^{-1})$ is the

desired regulation dynamics. The controller parameters in Equation (4.12) are calculated directly from the estimates of $A(z^{-1})$ and $B(z^{-1})$. These, in turn, are calculated by the RLS on-line estimation algorithm. Since the controller does not cancel the process zero polynomial $B(z^{-1})$, non-minimum phase processes can be controlled.

It can be seen from Figure 4.2 that the control signal is computed as:

$$u(k) = \frac{A(z^{-1})}{bC_r(z^{-1}) - z^{-d}B(z^{-1})}[C_r(z^{-1})y_{ref} - y(k)] \tag{4.13}$$

For the end milling process, the orders of $A(z^{-1})$ and $B(z^{-1})$, n_a and n_b, are both equal to 1.

A second-order regulation dynamics (Tomizuka et al., 1983; Kim and Huang, 1992; etc.) is chosen:

$$C_r(z^{-1}) = 1 + c_1 z^{-1} + c_2 z^{-2} \tag{4.14}$$

The control law for the end milling process can be obtained from Equation (4.13):

$$\begin{aligned} u(k) = [&(1+a_1)(1+c_1+c_2)y_{ref} - y(k) - a_1 y(k-1) + b_0 u(k-d) + b_1 u(k-d-1) \\ &- bc_1 u(k-1) - bc_2 u(k-2)]/b \end{aligned} \tag{4.15}$$

with $b = b_0 + b_1$.

4.3.2 Simulation Studies

The DB MRAC was simulated for spindle power and cutting force control of the end milling process. The simulated cutting conditions given in Section 4.2 were used. The process parameters of the spindle power and cutting force systems under this condition can be found in Tables 4.1 and 4.2. The regulation dynamics polynomials were

selected based on simulation results to provide reasonable overshoot and settling time without excessive control oscillation.

Power adaptive control

The algorithm was first tested with a noise-free case. The initial feedrate and spindle power were set to 0 and 0.1 HP respectively. Simulation results with the regulation dynamics $C_r(z^{-1}) = 1 - 0.3z^{-1} + 0.06z^{-2}$, as shown in Figure 4.3, were found to be very satisfactory. Figure 4.3(a) shows that the spindle power is well regulated with the settling time and overshoots being about 4 seconds and 0.1 HP respectively. In about two seconds after the start-up or the depth of cut changes, the estimates of the process parameters converge to the new values (Figure 4.3(c) and (d)) and the feedrate is brought to the steady-state values (Figure 4.3(b)).

To simulate the performance of the controller with noisy process measurements, a random noise with a mean of zero and a variance of 0.005 was added to the spindle power output. The rest of the simulation conditions were the same as those of the noise-free studies. Simulation results are shown in Figure 4.4. As shown in Figure 4.4(a), the spindle power is still well regulated around the desired reference level. The power response converges to its steady-state value faster than that of noise-free case with little oscillation, which can be explained by the increasing input excitation. Some spikes occur in feedrate but they are eliminated quickly (Figure 4.4(b)). The estimates of the process parameters oscillate but do not deviate much from the given values (Figure 4.4(c) and (d)).

Force adaptive control

Again the noise-free case was tested first. The initial feedrate and cutting force output were all selected to be zero. Good results with regulation dynamics $C_r(z^{-1}) = 1 - 0.5z^{-1} + 0.02z^{-2}$ are shown in Figure 4.5. The force plot (Figure 4.5(a)) shows that the overshoots in force output at the time of depth of cut changes have an amplitude of 120 N. The force output resumes to the reference value within approximately 4 seconds, which is more sluggish than that experienced with the power transients in power adaptive control. In 2 seconds, the feedrate adapts to the new values without much oscillation (Figure 4.5(b)) and the parameter estimates converge (Figure 4.5(c) and (d)).

The algorithm was then tested under noisy measurement circumstances. A random noise with a mean of zero and a variance of 1.5 was added to the force output. The rest of the simulation conditions were the same as those of the noise-free simulations. Figure 4.6 shows the simulation results. As shown in the force and feedrate plots of Figure 4.6(a) and (b), it takes longer for feedrate commands and force output to converge to their respective steady-state values. The force overshoots have a larger amplitude of 200 N. Parameter estimates are oscillatory (Figure 4.6(c) and (d)) and some spikes exist in feedrate commands. However, the system stability is not disturbed.

Extensive simulations showed that the power and force control systems using DB MRAC scheme were stable over a large range of process parameters, although the transient and steady-state performance varied. By selecting suitable C_r, the desired system

dynamic characteristics could be tuned.

The longer the process delay time, the worse the controller's performance. However, the algorithm still offered satisfactory results to the adaptive control of the cutting force system which had a longer output time delay than the spindle power system.

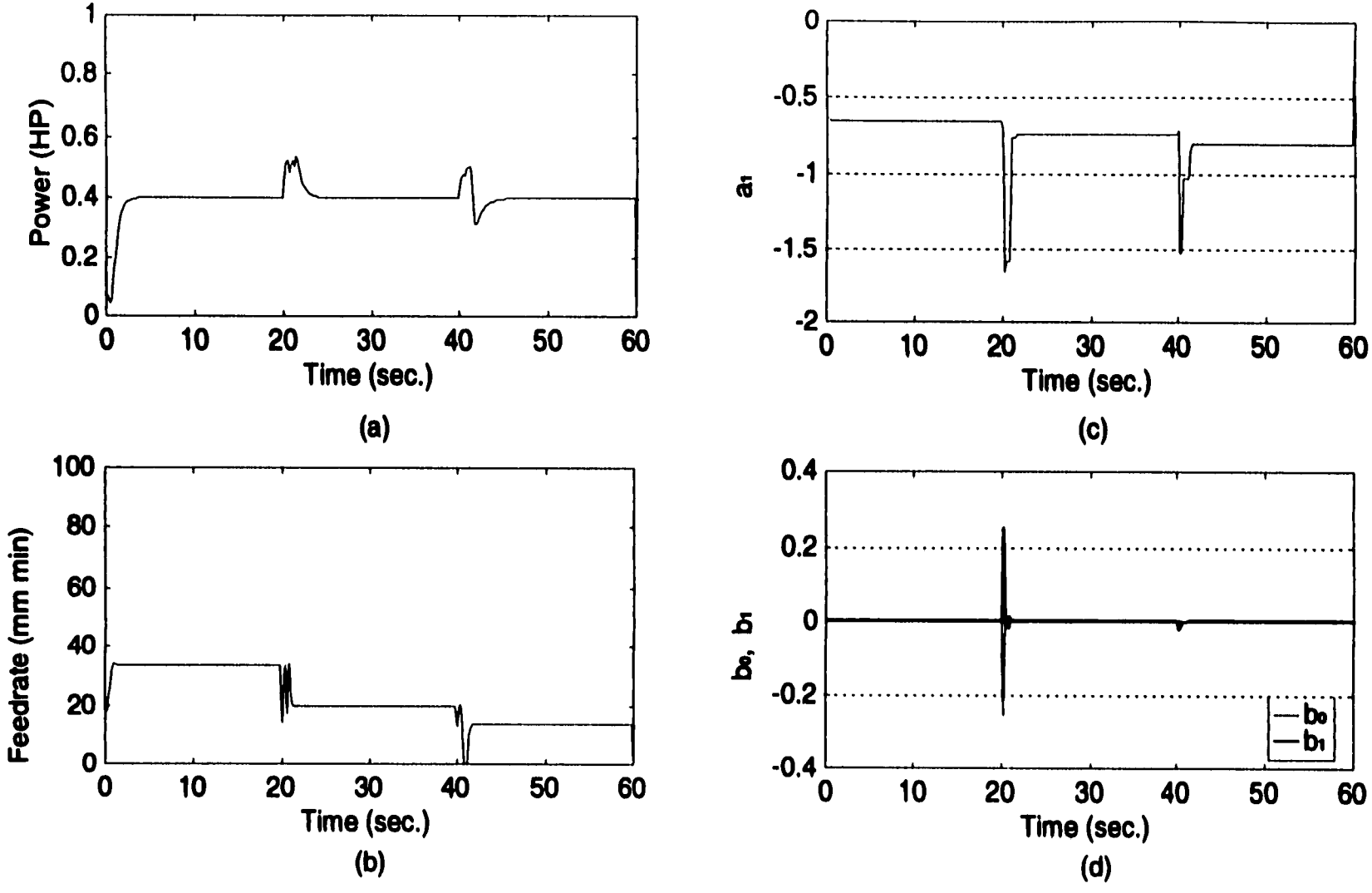

Figure 4.3 Simulation results of spindle power control using DB MRAC
(Without measurement noise)

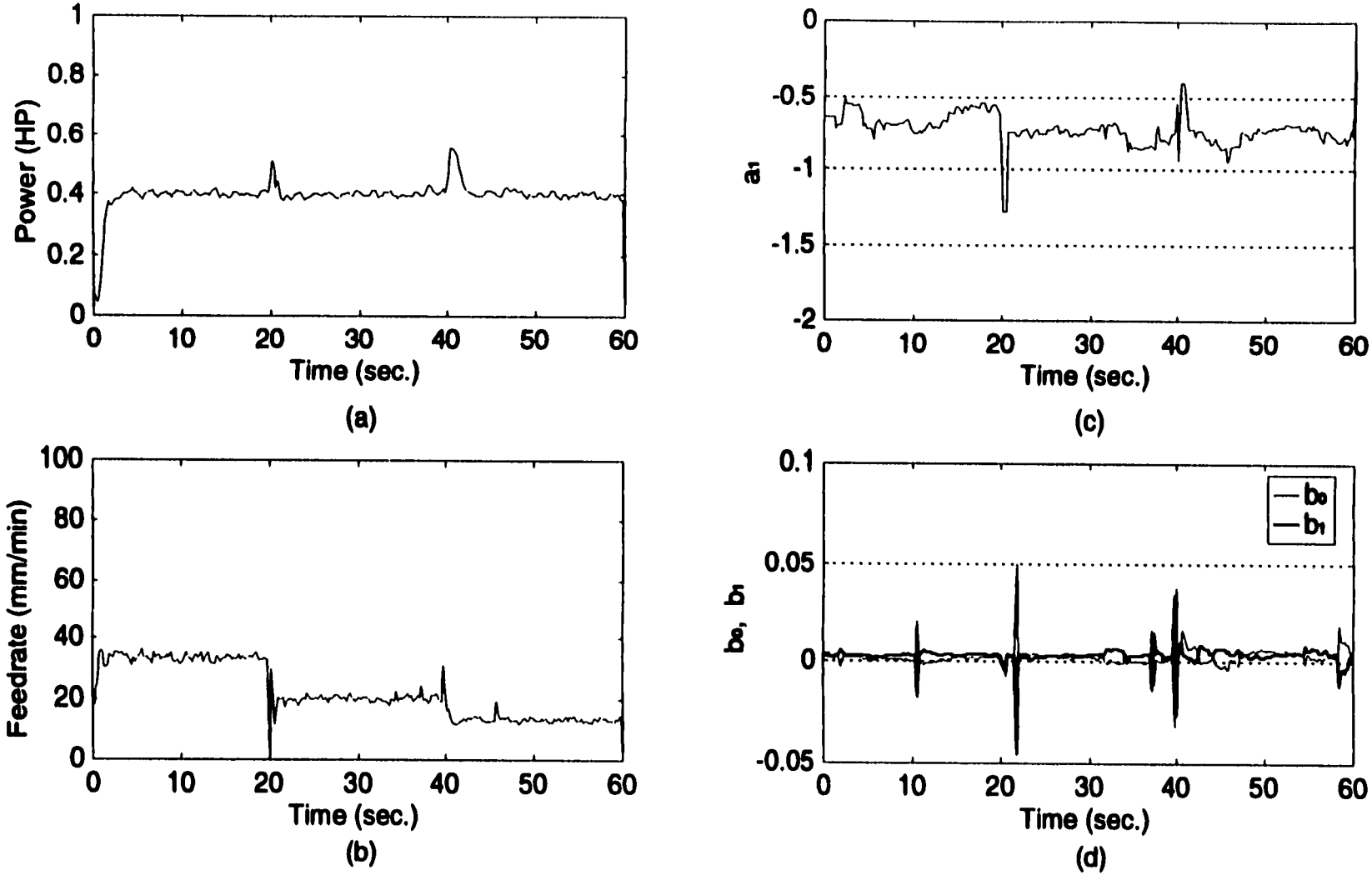

Figure 4.4 Simulation results of spindle power control using DB MRAC
(With measurement noise)

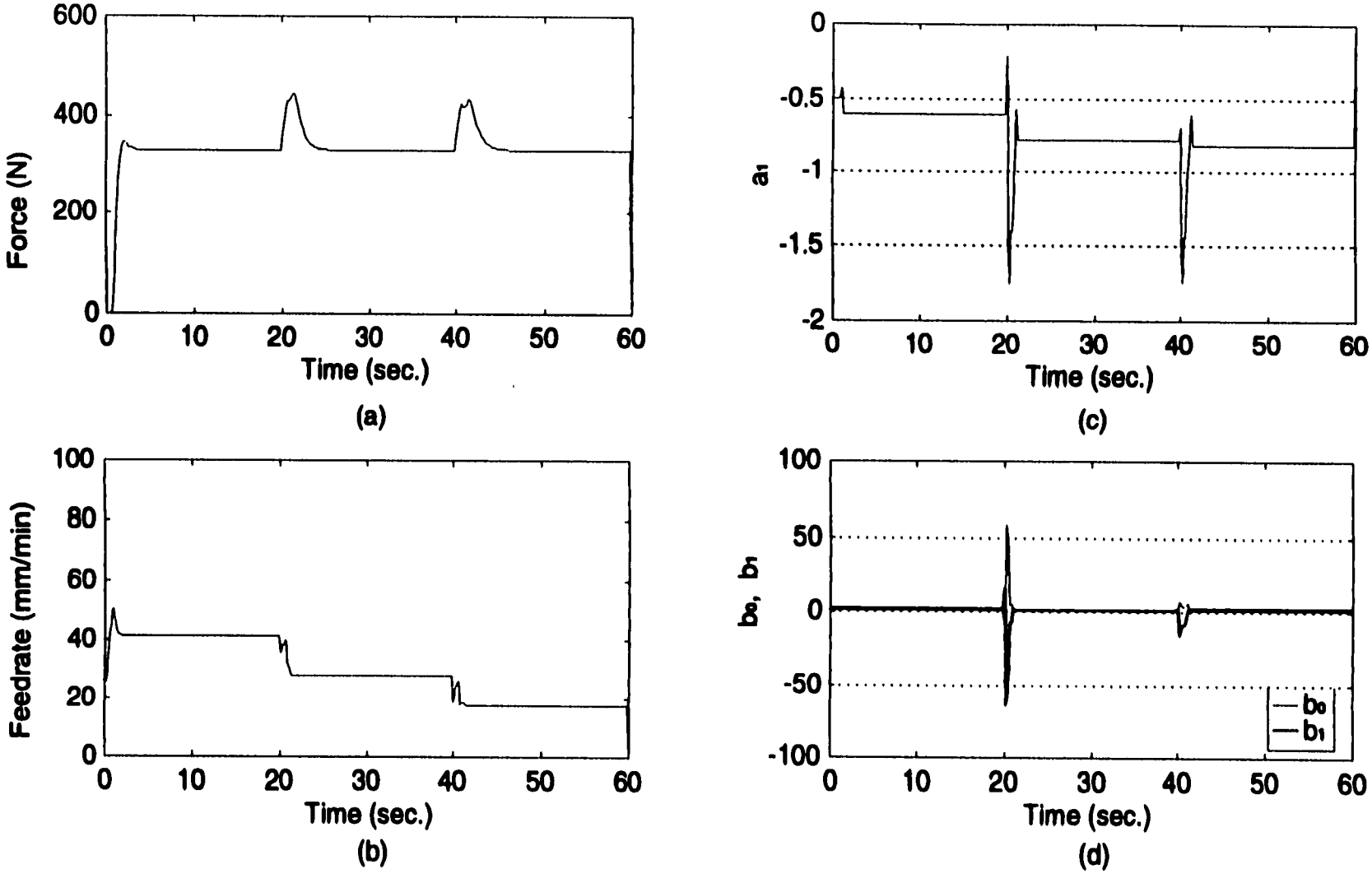

Figure 4.5 Simulation results of cutting force control using DB MRAC
(Without measurement noise)

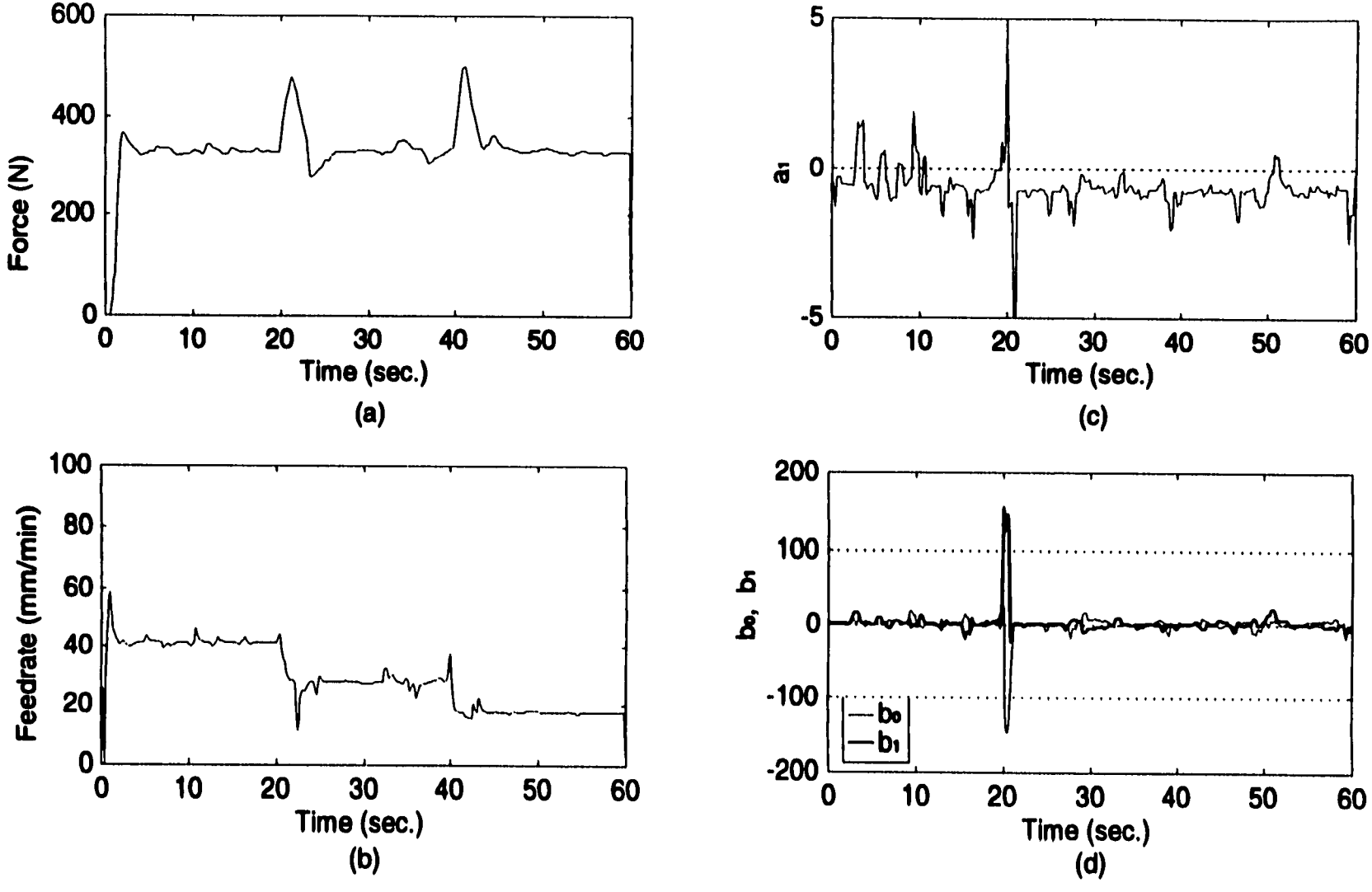

Figure 4.6 Simulation results of cutting force control using DB MRAC
(With measurement noise)

4.4 Modified MRAC Scheme

4.4.1 Modified MRAC Design

This algorithm was developed by Liu and Liang (1989) on the basis of Landau and Lozano's ITR MRAC algorithm (Landau and Lozano, 1981). It avoids the presence of the process zero polynomials in the denominator of the controller transfer function. The structure of the modified MRAC is shown in Figure 4.7.

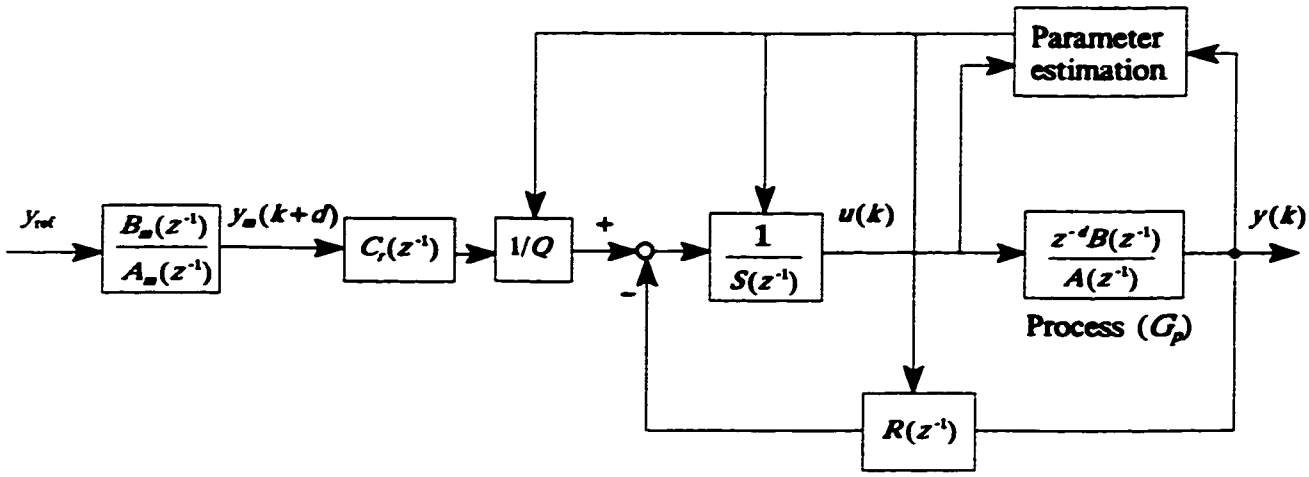

Figure 4.7 Structure of modified MRAC

For the plant depicted in Equation (4.9), the control law is:

$$u(k) = \frac{\frac{C_r(z^{-1})}{Q} y_{ref} - R(z^{-1})y(k)}{S(z^{-1})} \tag{4.16}$$

with $Q = \begin{cases} 1 & \text{when } B(1)=0 \\ B(1) & \text{when } B(1)\neq 0 \end{cases}$

$$C_r(z^{-1}) = 1+c_1z^{-1}+c_2z^{-2}+\cdots+c_{n_c}z^{-n_c}$$

$$R(z^{-1}) = r_0+r_1z^{-1}+r_2z^{-2}+\cdots+r_{n_a-1}z^{-(n_a-1)}$$

$$S(z^{-1}) = 1+s_1z^{-1}+s_2z^{-2}+\cdots+s_{n_b+d-1}z^{-(n_b+d-1)}.$$

The parameter Q normalizes the steady state controller gain to ensure that the controlled variable follows the desired output at steady state. $C_r(z^{-1})$ is the regulation dynamics with the highest order $n_c = n_a+n_b+d-1$. $R(z^{-1})$ and $S(z^{-1})$ are the controller parameter polynomials and can be determined from the Bezout identity (Liu and Liang, 1989):

$$C_r(z^{-1}) = z^{-d}B(z^{-1})R(z^{-1}) + S(z^{-1})A(z^{-1}) \tag{4.17}$$

The reference model has the same form as Equation (4.10). Since constant spindle power or cutting force level y_{ref} are desired, the $A_m(z^{-1})$ and $B_m(z^{-1})$ are selected to be 1. Thus $y_m(k+d)$ and y_{ref} are identical, as shown in Equation (4.11).

For second-order regulation dynamics (Equation (4.14)), the control laws for the control of the end milling process with different time delays can be derived from Equation (4.16) as shown below:

<u>Power control (d=2)</u>

$$u(k) = (1+c_1+c_2)y_{ref}/Q - s_1u(k-2) - s_2u(k-3) - r_0y(k) \tag{4.18}$$

with

$$\begin{bmatrix} s_1 \\ s_2 \\ r_0 \end{bmatrix} = \begin{bmatrix} 1 & 0 & 0 \\ a_1 & 1 & b_0 \\ 0 & a_1 & b_1 \end{bmatrix}^{-1} \begin{bmatrix} c_1-a_1 \\ c_2 \\ 0 \end{bmatrix} \tag{4.19}$$

Force control (d=3)

$$u(k) = (1+c_1+c_2)y_{ref}/Q - s_1u(k-3) - s_2u(k-4) - s_3u(k-5) - r_0y(k) \tag{4.20}$$

with

$$\begin{bmatrix} s_1 \\ s_2 \\ s_3 \\ r_0 \end{bmatrix} = \begin{bmatrix} 1 & 0 & 0 & 0 \\ a_1 & 1 & 0 & 0 \\ 0 & a_1 & 1 & b_0 \\ 0 & 0 & a_1 & b_1 \end{bmatrix}^{-1} \begin{bmatrix} c_1 - a_1 \\ c_2 \\ 0 \\ 0 \end{bmatrix} \tag{4.21}$$

Since the process zero polynomial does not appear in the denominator of any transfer function, this algorithm can be applied to both minimum and non-minimum phase processes. The closed-loop characteristics can be specified by stable regulation dynamics.

4.4.2 Simulation Studies

The modified MRAC was simulated for spindle power and cutting force control of the milling process by using the same cutting conditions as those used in the simulation studies of the DB MRAC approach. The regulation dynamics polynomials were selected based on simulation results.

Power adaptive control

The system's responses were found to be highly dependent on the regulation dynamics characteristics and sensitive to process parameter variations. The stability was maintained only in a small range of regulation dynamics. Figure 4.8 shows relatively

good results with $C_r(z^{-1}) = 1 - 0.82z^{-1} + 0.07z^{-2}$. Although the estimation performs well (Figure 4.8(c) and (d)), the feedrate has large overshoots at transients (Figure 4.8(b)). The power overshoots when the depth of cut changes are in the range of 0.15 to 0.2 HP and the power transients last approximately 5 seconds (Figure 4.8(a)). Both values are larger than in the DB MRAC power control, indicating that the system has slower response and larger transient peaks than the power control system.

To evaluate the effects of the measurement noise on the controller performance, a random noise with a mean of zero and a variance of 0.005, which is the same as that used in the DB MRAC power control, was added to the spindle power output. The simulation results are shown in Figure 4.9. The performance is not acceptable since unbounded feedrate, large power overshoots and spikes are observed (Figure 4.9(a) and (b)). Estimates are oscillatory and biased (Figure 4.9(c) and (d)).

Force adaptive control

In the noise-free cutting force control, the system was found to be unstable for most regulation dynamics tried. Satisfactory simulation results with $C_r(z^{-1}) = 1 - 0.86z^{-1} + 0.01z^{-2}$ are shown in Figure 4.10. Compared with the simulation results of cutting force control using the DB MRAC, the feedrate command and force output all exhibit much longer settling times in transients (Figure 4.10(a) and (b)).

Figure 4.11 shows the simulation results of cutting force control under a noisy measuring environment. A random noise with a mean of zero and a variance of 1.5 was added to the cutting force output. The system become unstable (Figure 4.11(a) and (b))

and the estimates are oscillatory and biased (Figure 4.11(c) and (d)).

Extensive simulations were carried out and it was found that the modified MRAC scheme was very sensitive to process parameter variations. It was difficult to tune to achieve satisfactory results for both power and force control systems.

4.5 Summary of Adaptive Controller Evaluation

The above simulation studies have shown that the DB MRAC can be successfully applied to the end milling process for spindle power and cutting force control. The controller yields a stable and quick response over a wide range of cutting conditions. Compared with the modified MRAC, it is simple to design and implement. The control law can be constructed directly from the estimates of the process parameters. It can be easily tuned to achieve desired transient and steady-state characteristics.

Simulation results have indicated that the modified MRAC algorithm has poorer performance than the DB MRAC for power and force control of the end milling process studied in this research, especially in force control where a longer time delay exists. Since the calculation of controller parameters from process parameter estimates is involved in the modified MRAC design and the number of controller parameters increases with the process time delay, the sensitivity of the modified MRAC's performance to the regulation dynamics and cutting condition variations can be expected. Such indirect adaptive schemes are suitable only for the systems with a low order model. For the control of systems containing a substantial time delay, the design complexity,

computing time and memory requirements will escalate rapidly as the order of the system model becomes higher and the number of controller parameters increases. The adaptive capability of the controller will also be undermined.

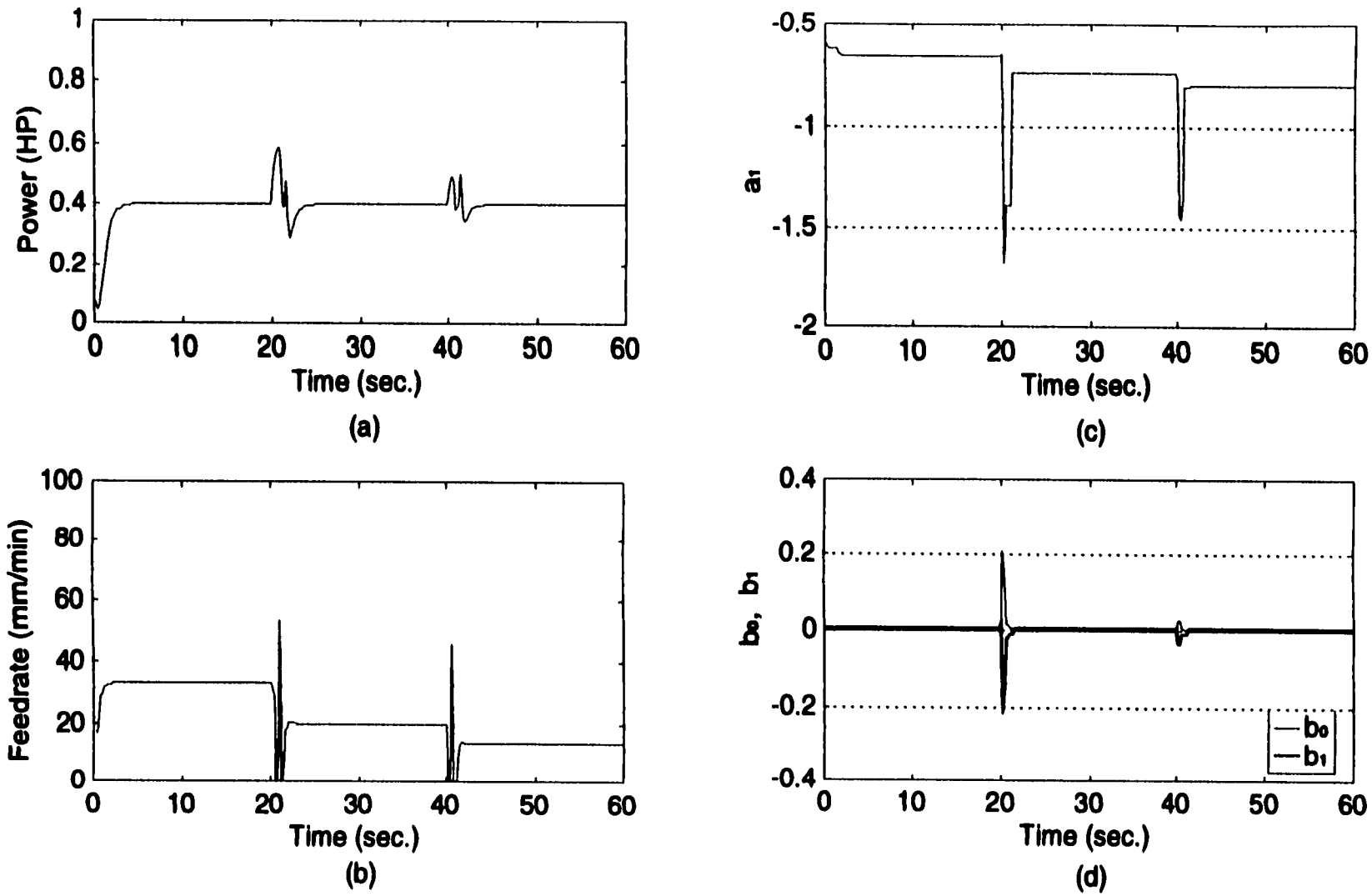

Figure 4.8 Simulation results of spindle power control using modified MRAC
(Without measurement noise)

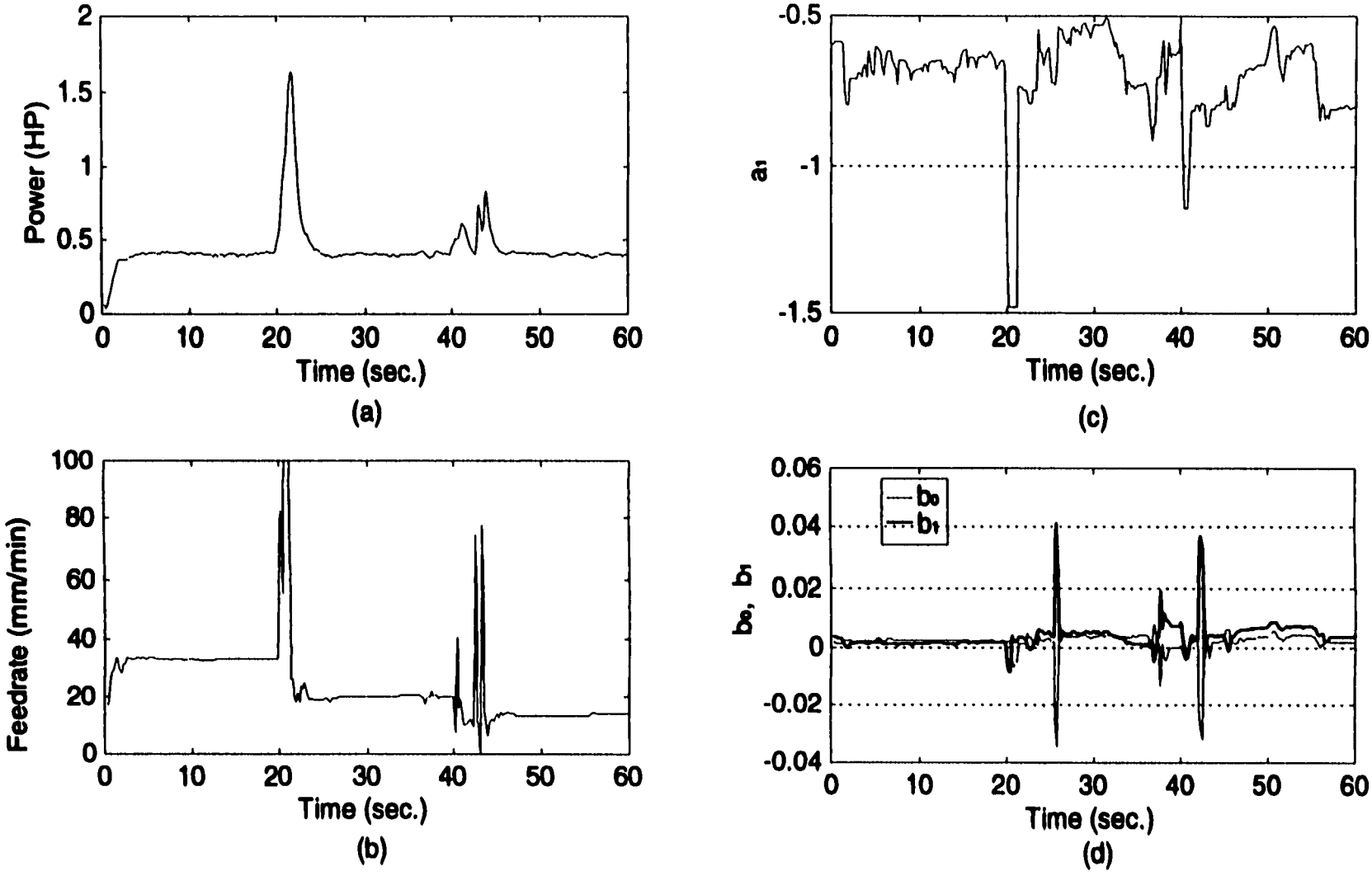

Figure 4.9 Simulation results of spindle power control using modified MRAC
(With measurement noise)

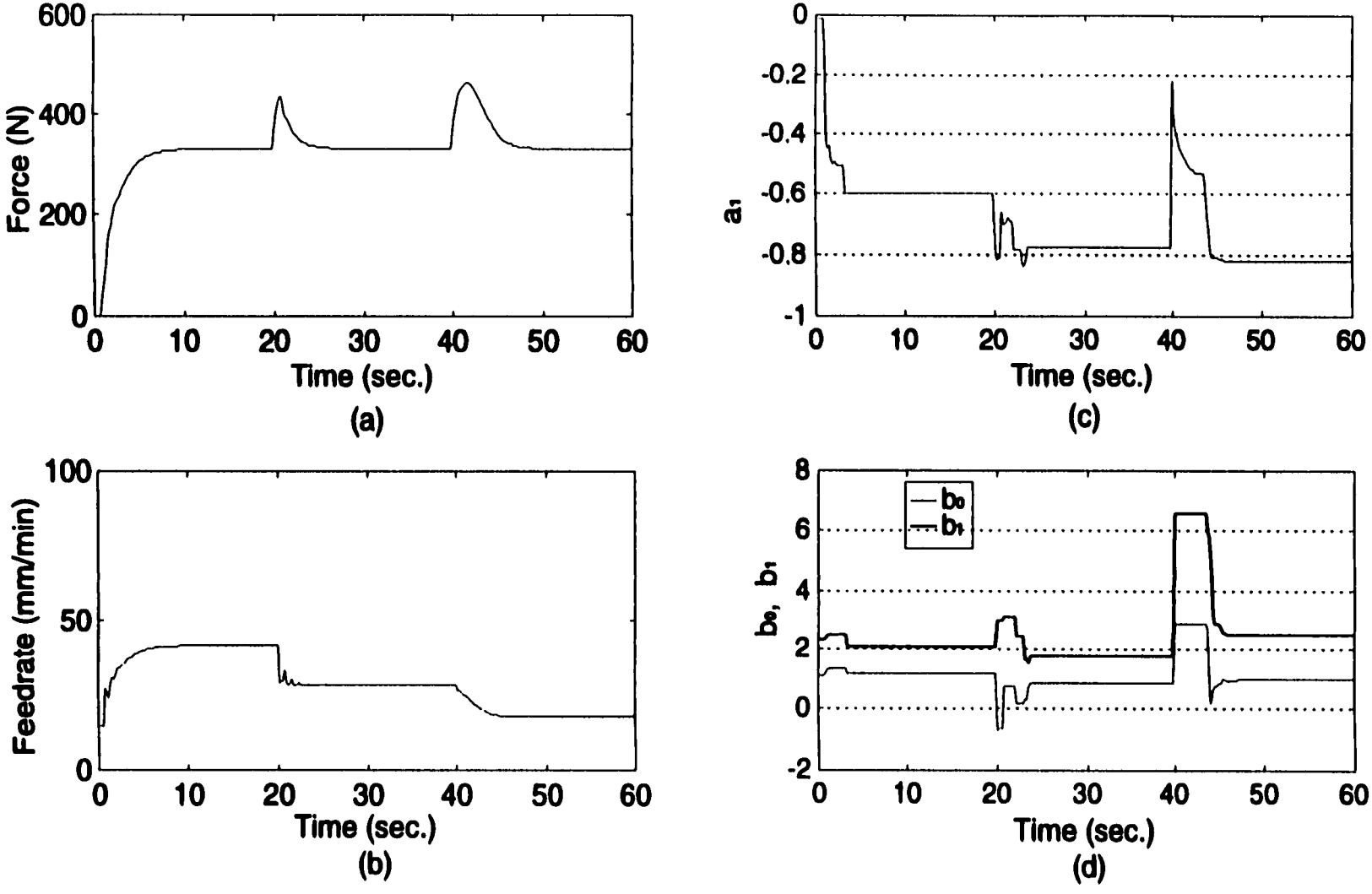

Figure 4.10 Simulation results of cutting force control using modidfied MRAC (Without measurement noise)

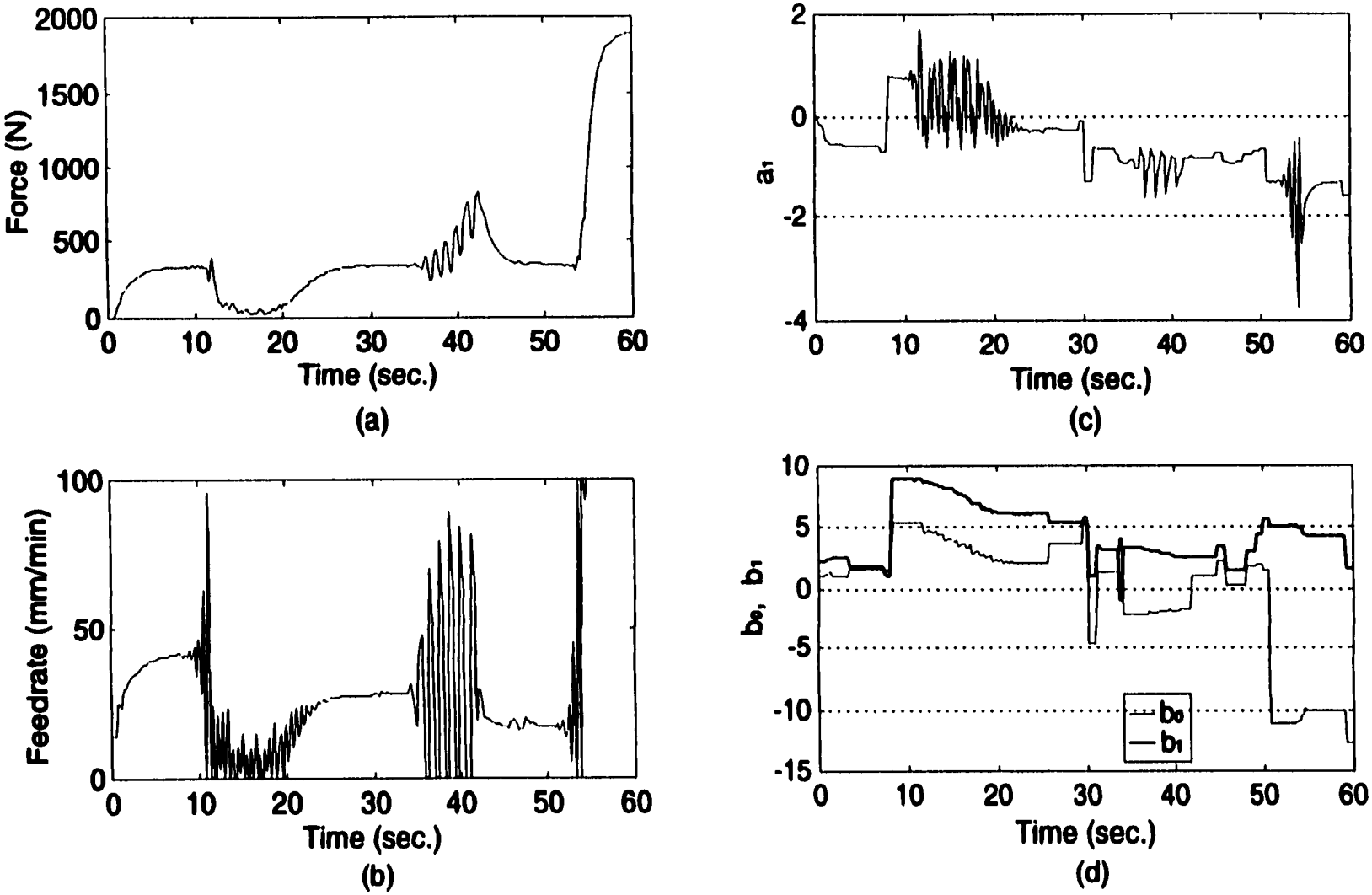

Figure 4.11 Simulation results of cutting force control using modified MRAC
(With measurement noise)

Chapter 5

Experimental Results of Power and Force Adaptive Control Using DB MRAC

The simulation studies in the previous chapter have shown that the DB MRAC is capable of controlling spindle power and cutting force in the end milling process with good performance. In this chapter, the implementation of the DB MRAC algorithm for spindle power and cutting force adaptive control in the end milling process is conducted.

5.1 Experimental Setups for Power and Force Adaptive Control

Experimental evaluation of the DB MRAC algorithm was conducted on the experimental setups depicted in Section 3.1. HSS 14.3 mm end milling cutters with four helical flutes and 30° helix angles were used. Slot milling without coolant along *Y*-axis was performed on C1018 cold rolled steel workpieces which were prefabricated with profiles as shown in Figure 5.1. The spindle speed was 300 rpm.

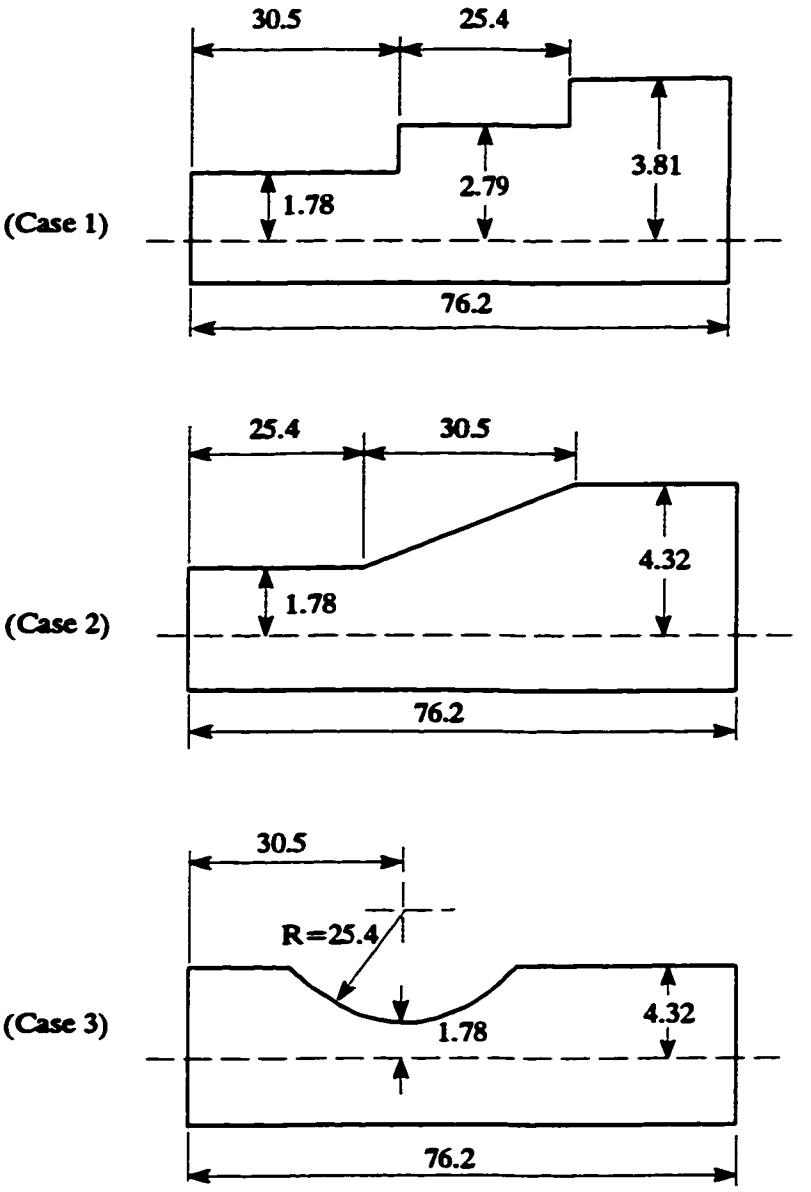

Figure 5.1 Geometries of the workpieces (unit: mm)

5.2 Results of Adaptive Control Experiments

The reference levels of spindle power and cutting force were set to 0.4 HP and 330 N respectively, same as the ones used in the simulation studies. The feedrate was adjusted by the control algorithm to maintain a desired reference level for spindle power or cutting force. The feedrate commands (in percentage of full scale feedrate) were calculated by the control algorithm, based on the digitalized voltage data of the filtered power or force measurements. To avoid tool damage, the maximum feedrate was set at 100 mm/min. A minimum feedrate of 5 mm/min was also set to avoid cutter rubbing on the workpiece surface. The initial feedrate was selected so that the power or force output was lower and close to the specified reference values.

The selection of the sampling intervals has critical effect on system performance. Generally, faster sampling allows more accurate model tracking. However, too small a sampling interval will increase the process delay steps d, thus resulting in much deteriorated control performance. When the sampling interval is too large, system tracking cannot be satisfied. In the following experiments, suitable sampling intervals were selected based on the performance of the actual control tests.

The control programs were coded in Borland C++ language. The execution time for the estimation and control calculations at each sampling period is about 3 milliseconds. The program listing is given in Appendix D.

5.2.1 Power Adaptive Control

According to the simulation studies of power adaptive control in Section 4.3.2,

the regulation dynamics polynomial was chosen as $C_r(z^{-1}) = 1 - 0.3z^{-1} + 0.06z^{-2}$.

The sampling interval of 0.2 seconds was initially used but failed to yield stable control performance. Based on the cutting tests using different sampling frequencies, the sampling interval of 0.25 seconds was selected, still leading to a two-point delay model for power control system, i.e., d=2.

Experimental results on the three different workpieces are shown in Figures 5.2 to 5.4.

For all the three cases, it can be seen from the b_0 and b_1 plots (Figure 5.2(d), 5.3(d) and 5.4(d)) that b_1 is greater than b_0, so that the ratio of b_1/b_0 is greater than one. Therefore the spindle power control system is non-minimum phase.

Case 1, step changes of depth of cut (Figure 5.2)

It is seen from the power plot shown in Figure 5.2(a) that the spindle power is well regulated around the desired value. The power transients are very smooth and no significant overshoots occur. Figure 5.2(b) shows that the input feedrate also settles to the new values smoothly during the periods of depth of cut change. The responses are smoother than those in simulation studies due to the gradual cutting condition variations in real cutting.

As displayed in Figure 5.2(c) and (d), the estimates of a_1, b_0 and b_1 exhibit oscillations, which are particularly severe at low depths of cut. This could be caused by lack of input richness and unmodelled dynamics due to measurement noise. As the depth of cut increases, the estimates, especially that of a_1, converge to their true values,

indicating the increasing excitation of the system. In the feedrate plot (Figure 5.2(b)), the initial overshoots and the bursts at the first depth of cut change can all be related to the biased estimates in the transients of the parameter estimation (Fussell and Srinivasan, 1991).

Case 2, sloping change of depth of cut (Figure 5.3)

Again a good power regulation is achieved (Figure 5.3(a)). The feedrate decreases smoothly as the depth of cut increases (Figure 5.3(b)). The estimates of a_1, b_0 and b_1 are oscillatory at low depths of cut (Figure 5.3(c) and (d)). This causes the feedrate bursts at the early stage of control (Figure 5.3(b)). The system performs better as the estimation improves at higher depths of cut.

Case 3, curved change of depth of cut (Figure 5.4)

Both the spindle power and the input feedrate respond smoothly (Figure 5.4(a) and (b)). There are only small feedrate bursts which impose no significant jump in the spindle power. a_1 has correct estimates except at low depths of cut (Figure 5.4(c)). The estimates of b_0 and b_1 are oscillatory (Figure 5.4(d)).

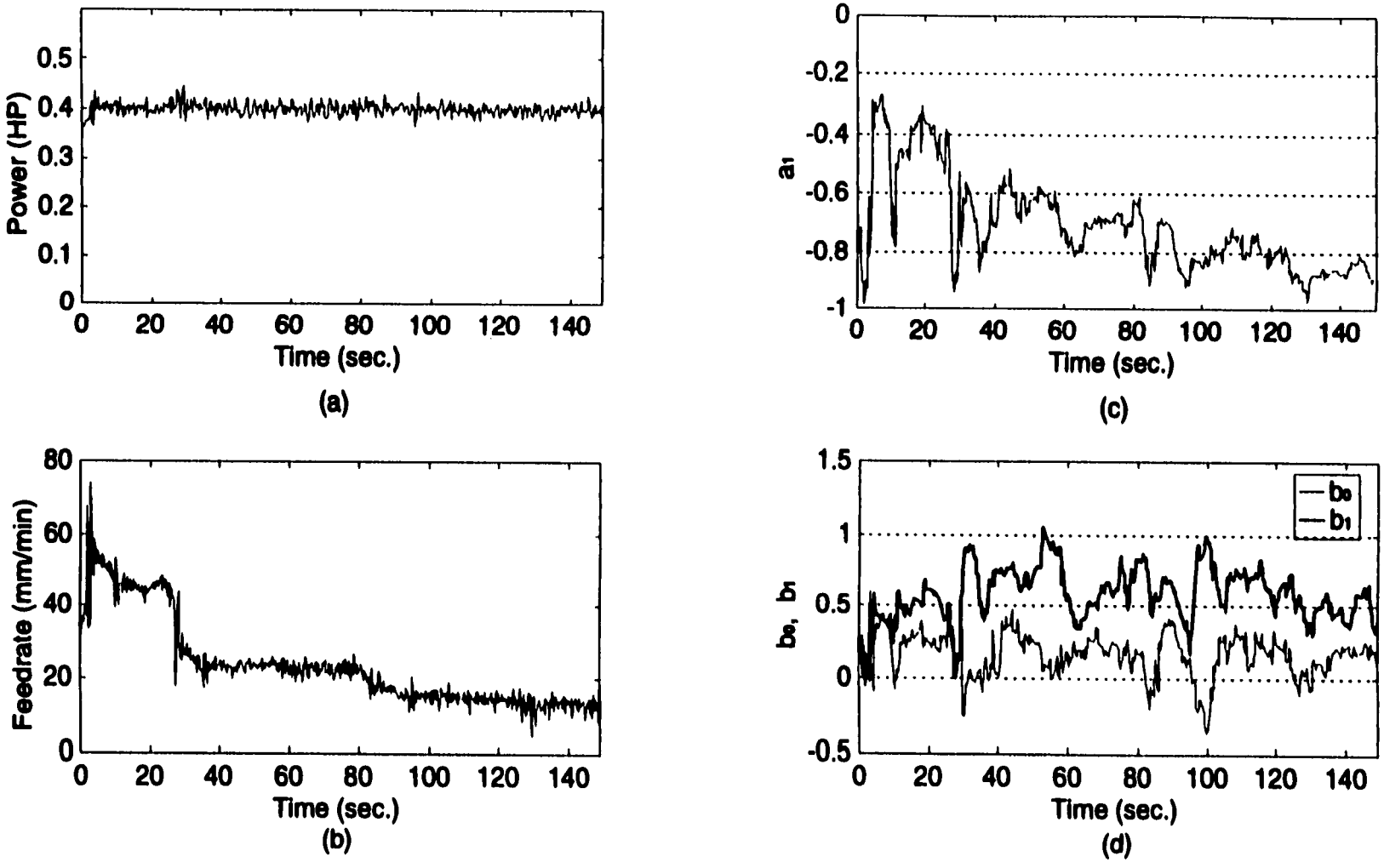

Figure 5.2 Experimental results of spindle power adaptive control (Case 1)

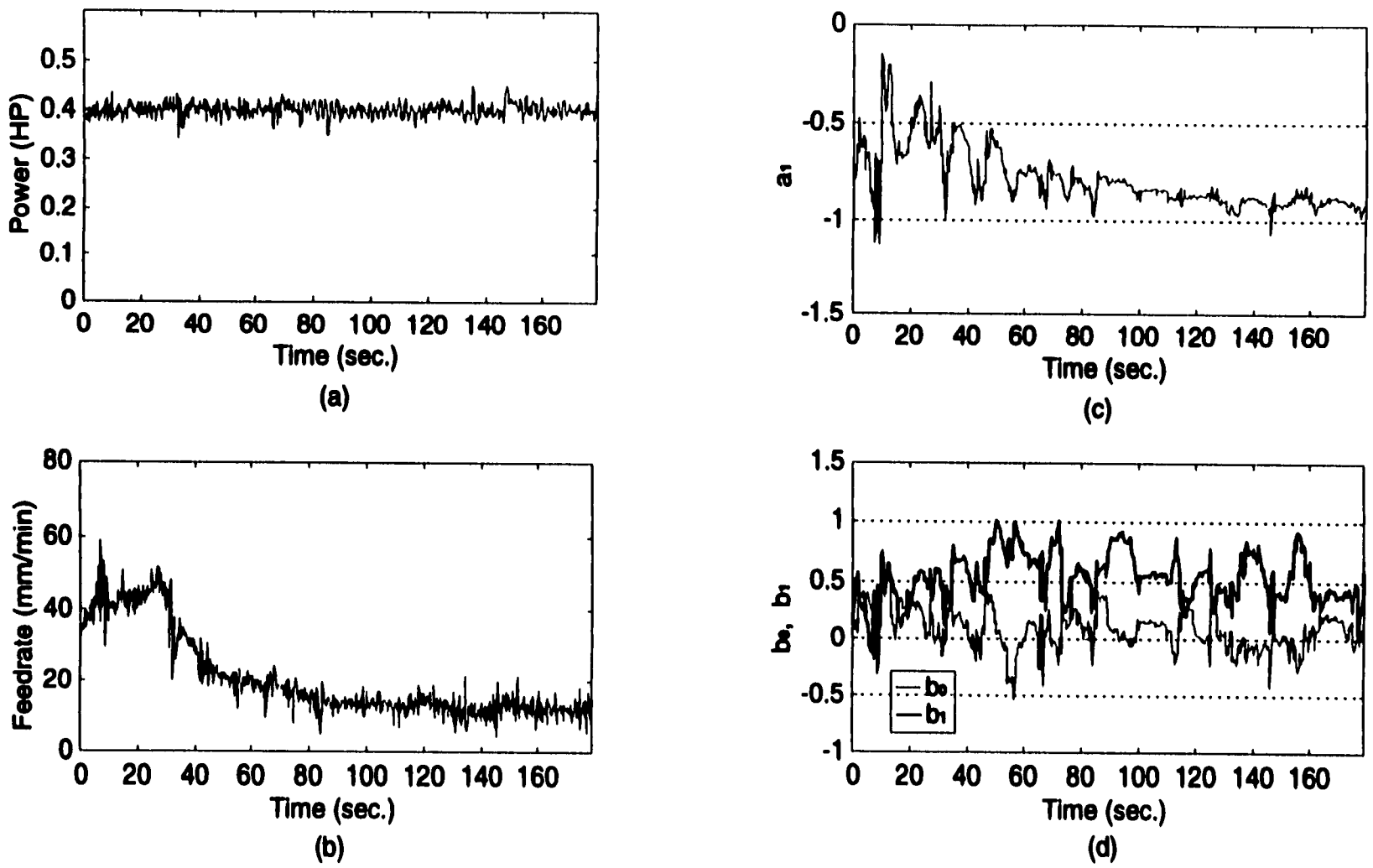

Figure 5.3 Experimental results of spindle power adaptive control (Case 2)

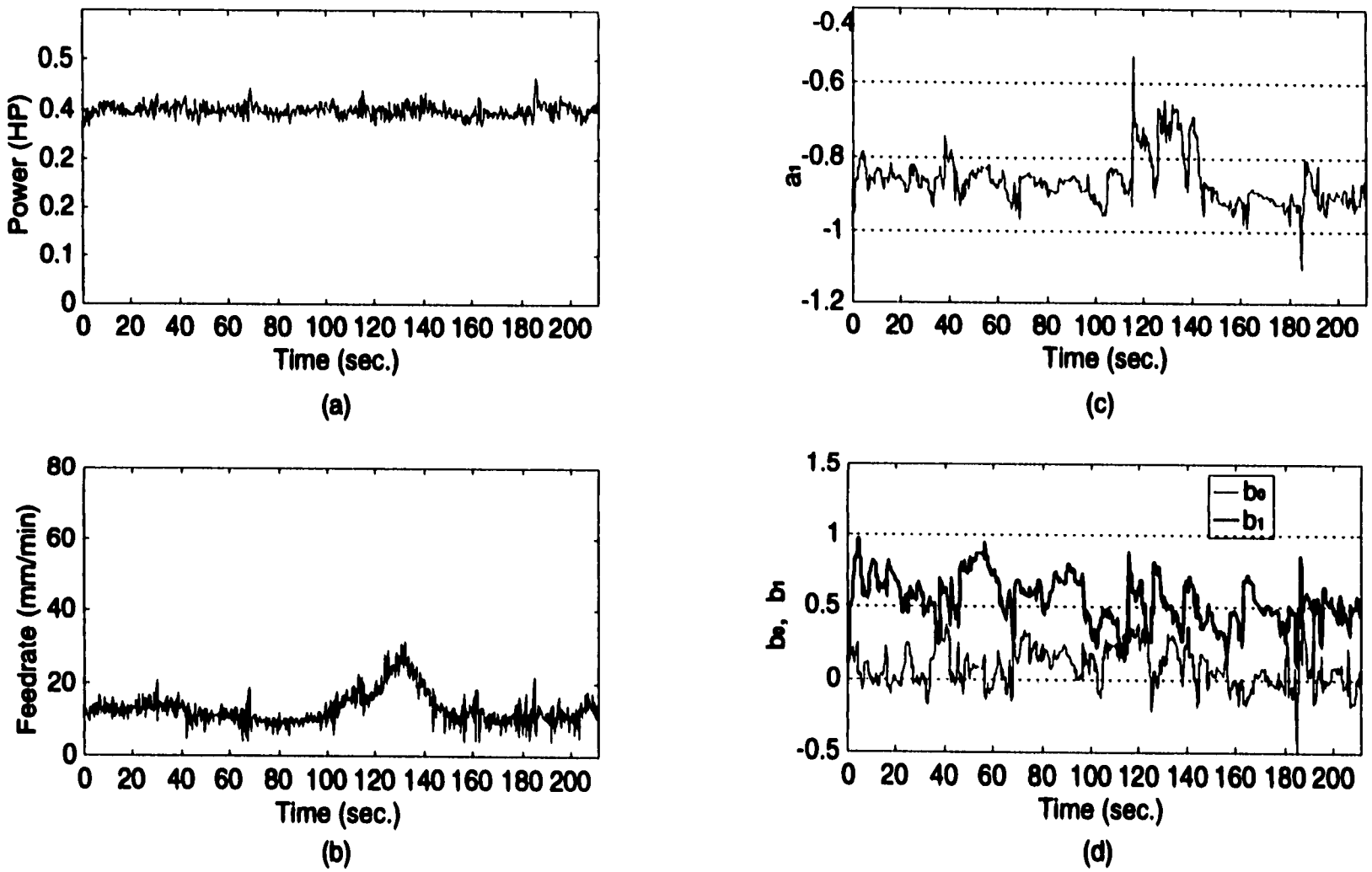

Figure 5.4 Experimental results of spindle power adaptive control (Case 3)

5.2.2 Force Adaptive Control

From the simulation studies of force adaptive control in Section 4.3.2, the regulation dynamics polynomial was selected as $C_r(z^{-1}) = 1 - 0.5z^{-1} + 0.02z^{-2}$.

The performance of force control with the sampling interval setting to 0.2 seconds was poor. By trying different values of sampling interval in the cutting tests, the sampling interval was selected to be 0.225 seconds, still leading to a three-point delay model for force control system, i.e., d=3.

Experimental results on the three different workpieces are shown in Figures 5.5 to 5.7.

From the b_0 and b_1 plots of all the three cases, Figure 5.5(d), 5.6(d) and 5.7(d), it is obvious that b_1 is less than b_0, thus the ratio of b_1/b_0 is less than one. Therefore the force control system is minimum phase.

Case 1, step change of depth of cut (Figure 5.5)

The cutting force is maintained around the reference value (Figure 5.5(a)). The force transients are fast with force overshoots with a magnitude of about 150 N. The feedrate has overshoots of about 15 mm/min (Figure 5.5(b)). Such performance is worse than the spindle power control counterpart discussed in Section 5.2.1(1). This can be attributed to the fact that the cutting force system has a longer time delay than spindle power system.

The estimation performs better at high depths of cut where the estimates converge to constant values (Figure 5.5(c) and (d)). As a result, the feedrate commands are

smoother at the highest depth of cut than at the lowest depth of cut (Figure 5.5(b)). The initial cutting force and feedrate overshoots are still present due to the transients of the estimation.

Case 2, sloping change of depth of cut (Figure 5.6)

The cutting force is well maintained around the reference value (Figure 5.6(a)). The response of input feedrate is smooth (Figure 5.6(b)). Only small bursts occur when the estimates are biased (Figure 5.6(c) and (d)). At high depths of cut, as the estimates converge, the feedrate commands become smoother.

Case 3, curved change of depth of cut (Figure 5.7)

The cutting force is well maintained at the desired level (Figure 5.7(a)). Feedrate commands perform smoothly at high and constant depths of cut (Figure 5.7(b)). The estimates turn out to be oscillatory when the depth of cut is small (Figure 5.7(c) and (d)), causing bursts in the feedrate commands and cutting force output (Figure 5.7(a) and (b)).

5.3 Summary of Experimental Results

Both spindle power and cutting force control systems of the end milling process had good transient and steady-state behaviours for different cutting conditions in actual control tests. Spindle power control performed better in the experiments than did the cutting force control and demonstrated smoother power transient responses. The reason is likely due to the shorter time delay of the spindle power system.

The spindle power output was maintained well at the desired level in the tests, implying that the cutting process was stable and the cutting load stayed at a constant level. This proves that the spindle power control scheme is feasible and is a very promising alternative for adaptive control of end milling processes.

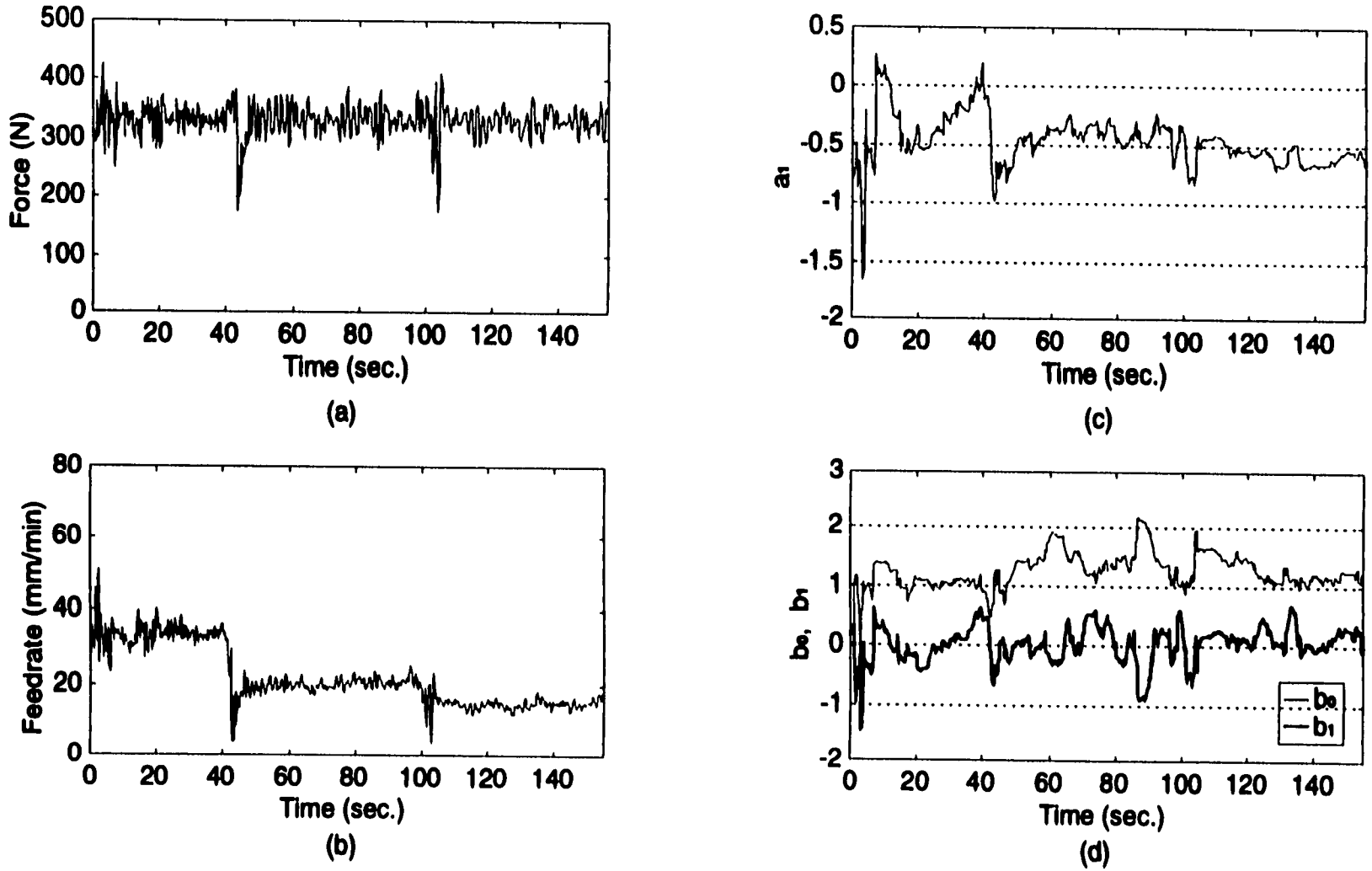

Figure 5.5 Experimental results of cutting force adaptive control (Case 1)

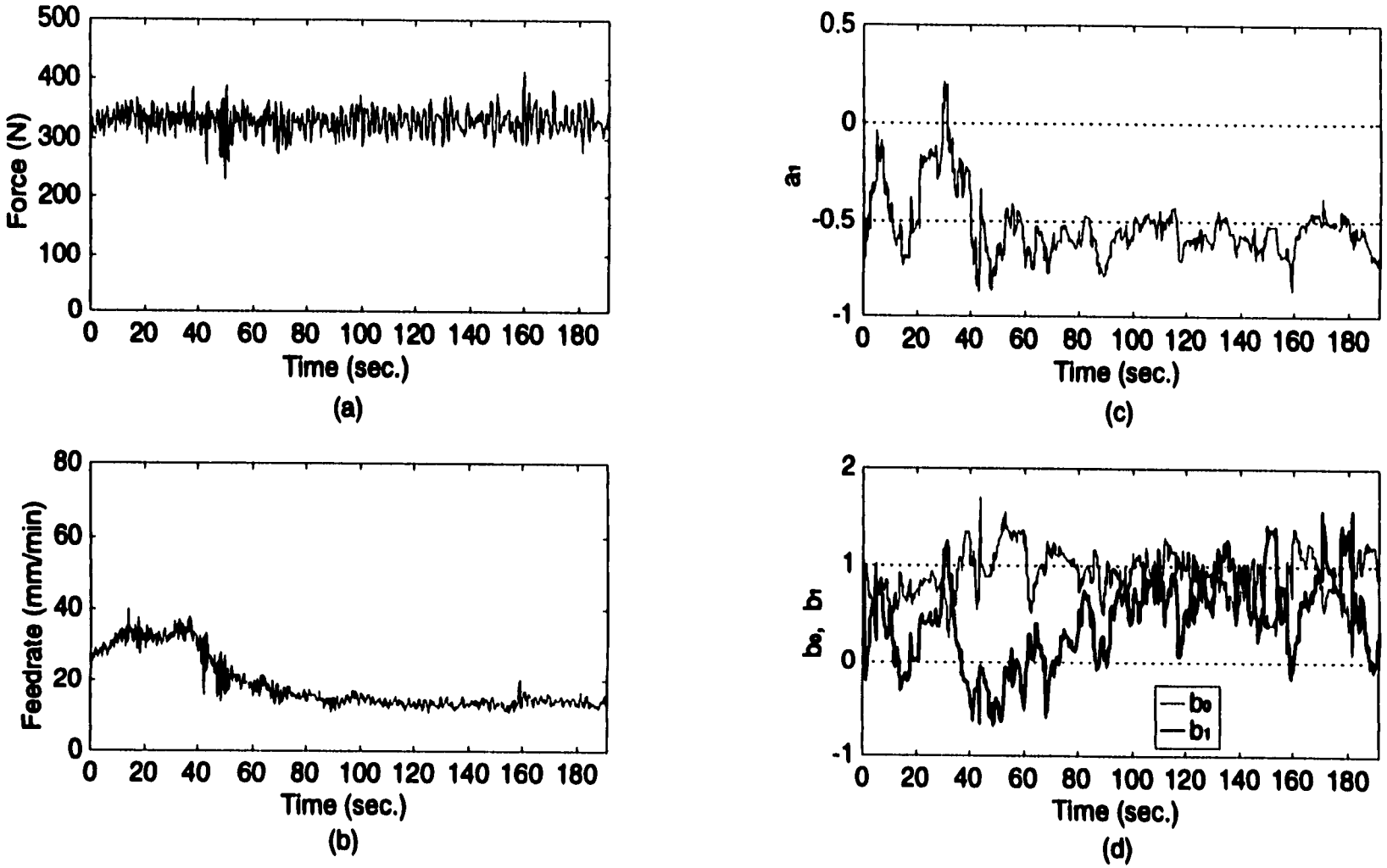

Figure 5.6 Experimental results of cutting force adaptive control (Case 2)

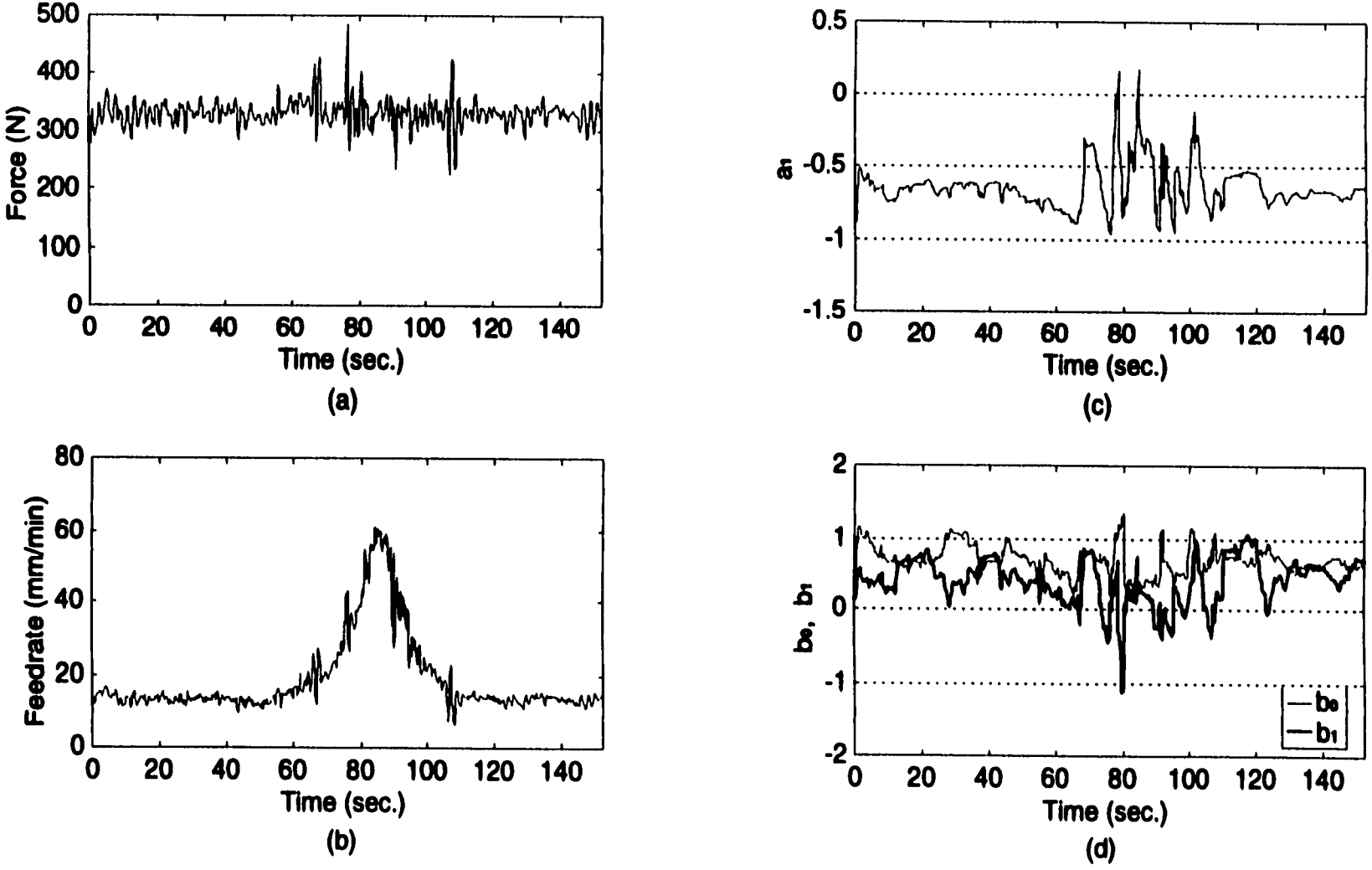

Figure 5.7 Experimental results of cutting force adaptive control (Case 3)

Chapter 6

Conclusions and Future Research

6.1 Conclusions

The purpose of this research was to develop and implement spindle power and cutting force adaptive control systems for the end milling process. To accomplish this, this thesis presents: (a) the development and experimental validation of the end milling process model for controller design, (b) the simulation evaluation of the DB MRAC and the modified MRAC algorithms, and © the implementation of the DB MRAC scheme for spindle power and cutting force control in the end milling process.

The major conclusions of this work are summarized below:

1. From the dynamic analysis of feed drive, spindle drive and cutting process, as well as the input and output samples of process identification experiments, a first-order model structure was found to be appropriate to describe the dynamics of the end milling process for steady-state cutting conditions and changes in the axial depth of cut.
2. The process parameters identified by the open-loop cutting experiments were found to vary significantly with cutting conditions. With the process time

delay being considered in the model, the resulting end milling process can be a non-minimum phase system.

3. Simulation studies showed that the DB MRAC had superior transient and steady-state performance in power and force adaptive control of the end milling process. The modified MRAC was shown to be sensitive to process parameter variations and to have poor behaviour when applied in the process.
4. The DB MRAC scheme gave very good transient and steady-state performance for a variety of cutting conditions in actual cutting tests in which power and force adaptive control was used in the end milling process. This demonstrated that the DB MRAC approach is effective in adaptive control of non-minimum and minimum phase end milling processes.
5. The great potential of power control as an alternative in adaptive control of end milling processes was justified from the results of the control experiments.

6.2 Future Research

In this research, single-input-single-output adaptive control systems were shown to be effective in maintaining a constant spindle power or cutting force level by manipulating the feedrate in the end milling process. The cutting conditions were restricted to slot milling of steel workpieces with constant and relatively low spindle speeds. Some promising topics for future work related to this research are listed below:

1. Development of more accurate linear or non-linear process models, modification of the current controller or application of other adaptive control algorithms to improve the performance of the control scheme and cope with more complex cutting conditions (e.g., non-slot milling and spindle speed change) should be considered.
2. To avoid trial and error in the selection of the on-line estimation and control parameters in real-time control, a scheme which is capable of systematically selecting these parameters is desirable.
3. Multiple-input-multiple-output adaptive control, e.g., regulating cutting loads and suppressing chatter simultaneously through manipulation of both feedrate and spindle speed, remains to be investigated for end milling process control. This scheme might be advantageous for further improvement of machining quality.

References

Altintas, Y., 1994, Direct Adaptive Control of End Milling Process, *International Journal of Machine Tools and Manufacturing*, Vol. 34, No. 4, pp. 461-472.

Astrom, K.J. and Wittenmark, B., 1990, *Computer-Controlled Systems*, Englewood Cliffs, New Jersey: Prentice Hall Inc.

Astrom, K.J. and Wittenmark, B., 1989, *Adaptive Control*, Reading, Massachusetts: Addison-Wesley Publishing Co.

Astrom, K.J., Hagander, P. and Sternby, J., 1984, Zeros of Sampled Systems, *Automatica*, Vol. 20, pp.31-38.

Baker, R.P.D. and Morris, A.J., 1985, A Generalised Minimum Variance Self-Tuning Controller for Systems with Large Dead Times, *Proceedings of the American Control Conference*, pp. 408-409.

Barthel, J.W. and Shin, Y.C., 1993, Adaptive Control of Nonminimum Phase Processes with Application to the End Milling Process, *Proceedings of the American Control Conference*, San Francisco, Cal., pp. 2449-2454.

Butler, H., Honderd, G. and Amerongen, J. van, 1990, Ripple-free model reference adaptive control, *Proceedings of 29th IEEE Conf. on decision and control*, Honolulu, Hawaii, pp. 1004-1009.

Butler, H., 1992, *Model Following Adaptive Control: From theory to practice*, Prentice Hall International(UK) Ltd.

Christian, E., 1983, *LC Filters: Design, Testing, and Manufacturing*, New York: John-Wiley & Sons Inc.

Cordero, A.O. and Mayne, D.Q., 1981, Deterministic Convergence of a Self-Tuning Regulator with Variable Forgetting Factor, *IEE proceedings*, Vol. 128, Part D, No. 1. pp. 19-23.

Daneshmend, L.K. and Pak, H.A., 1986, Model Reference Adaptive Control of Feed Force in Turning, *Journal of Dynamics Systems, Measurement, and Control*, Vol. 108, pp. 215-222.

Egardt, B., 1980, Unification of Some Discrete-Time Adaptive Control Schemes, *IEEE Transactions on Automatic Control*, Vol. AC-25, No. 4, pp. 693-697.

Elbestawi, M.A. and Sagherian, R., 1987, Parameter Adaptive Control in Peripheral Milling, *International Journal of Machine Tools and Manufacturing*, Vol. 27, No. 3, pp. 399-414.

Fortescure, T.R., Kershenbaum, L.S. and Ydstie, B.E., 1981, Implementation of Self-Tuning Regulators with Variable Forgetting Factors, *Automatica*, Vol. 17, No. 6, pp. 831-835.

Franklin, G.F., Powell, J.D. and Workman, M.L., 1990, *Digital Control of Dynamic Systems*, Reading, Massachusetts: Addison-Wesley Publishing Co.

Fussell, B.K. and Srinivasan, K., 1988, On-Line Identification of End Milling Process Parameters, *USA-Japan Symposium on Flexible Automation*, pp. 967-974.

Fussell, B.K. and Srinivasan, K., 1991, Adaptive Control of Force in End Milling Operations - An Evaluation of Available Algorithms, *Journal of Manufacturing systems*, Vol. 10, No. 1, pp. 8-20.

Fussell, B.K. and Srinivasan, K., 1988, Model Reference Adaptive Control of Force in End Milling Operations, *Proceedings of the America Control Conference*, pp. 1189-1194.

Fussell, B.K., 1987, *Modelling and Adaptive Force Control of End Milling Operations*, Ph.D. thesis, Ohio State University.

Garrett, P.H., 1994, *Advanced Instrumentation and Computer I/O Design: Real-Time System Computer Interface Engineering*, New York: IEEE Press.

Goodwin, G.C. and Sin, K.S., 1984, *Adaptive Filtering, Prediction and Control*, Englewood, New Jersey: Prentice-Hall Inc.

Hsu, Pau-Lo and Hsieh, Ming-Ying, 1994, Applications of Self-Tuning Control on Industrial CNC Machines, *International Journal of Machine Tools and Manufacturing*, Vol. 34, No. 6, pp. 859-877.

Huang, S.J. and Yan, M.T., 1993, Theoretical and Experimental Study of PI Control, Adaptive Control and Variable Structure Control for Converted Traditional Milling Machines, *International Journal of Machine Tools and Manufacturing*, Vol. 33, No. 5, pp. 695-712.

Isermann, R., 1989, *Digital Control Systems*, Vol. 1 & 2, Berlin: Springer-Verlag.

Isermann, R., Lachmann, K.-H. and Matko, D., 1992, *Adaptive Control Systems*, Prentice Hall International (UK) Ltd.

Isermann, R., 1982, Parameter Adaptive Control Algorithms - A Tutorial, *Automatica*, Vol. 18, No. 5, pp. 513-528.

Johnson, D.E., 1976, *Introduction to Filter Theory*, Eaglewood, New Jersey: Prentice-Hall Inc.

Julian, M., 1988, *Circuits, Signals & Devices*, Longman Group UK Ltd.

Jung, Chung-Young and Oh, Jun-Ho, 1991, Improvement of Surface Waviness by Cutting Force Control in Milling, *International Journal of Machine Tools and Manufacturing*, Vol. 31, No. 1, pp. 9-21.

Kim, K. and Huang, S.D., 1992, Implementation of Pole Placement Adaptive Controller for Force Control of Non-Minimum Phase End Milling Operations, *International Journal of Machine Tools and Manufacturing*, Vol. 32, No. 4, pp. 619-627.

Kistler Instrument Corporation, 1994, *Dual Mode Amplifier Type 5010A Operating Instructions*.

Kistler Instrument Corporation, 1993, *3-Component Dynamometer Type 9257B, Calibration Sheets*.

Kistler Instrument Corporation, 1993, *Quartz 3-Component Dynamometer Type 9257B Operating Instructions*.

Kistler Instrument Corporation, 1995, *Dual Mode Amplifier Model 5010A10, Certificates of Calibration*.

Kolarits, F.M. and DeVries, W.R., 1990, Adaptive Pole Placement Force Control of End Milling, *Proceedings of the American Control Conference*, pp. 1115-1120.

Kolarits, F.M., and DeVries, W.R., 1991, A Mechanistic Dynamic Model of End Milling for Process Controller Simulation, *ASME Journal of Engineering for Industry*, Vol. 113, pp. 176-183.

Koren, Y., 1983, *Computer Control of Manufacturing Systems*, New York: McGraw-Hill Book Co.

Koren, Y. and Masory, O., 1981, Adaptive Control with Process Estimation, *Annals of CIRP*, Vol. 30, No. 1, pp. 373-376.

Krause, P.C., 1986, *Analysis of Electric Machinery*, New York: McGraw-Hill Book Co.

Landau, I.D., 1993, Evolution of Adaptive Control, *Journal of Dynamic Systems, Measurements, and Control*. Vol. 115, pp. 381-391.

Landau, I.D. and Lozano, R., 1981, Unification of Discrete Time Explicit Model Reference Adaptive Control Designs, *Automatica*, Vol. 17, No. 4, pp. 593-611.

Laudau, I.D., 1979, *Adaptive Control: The Model Reference Approach*, New York: Marcel Dekker Inc.

Lauderbaugh, L.K. and Ulsoy, A.G., 1989, Model Reference Adaptive Force Control in Milling, *Journal of Engineering for Industry*. Vol. 111, pp. 13-21.

Lauderbaugh, L.K. and Ulsoy, A.G., 1988, Dynamic Modelling for Control of the Milling Process, *Journal of Engineering for Industry*, Vol. 110, pp. 367-375.

Lent, A.F. and Miastkowski, S., 1989, *Practical Applications Circuits Handbook*, San Diego, California: Academic Press.

Liu, M. and Liang, S., 1989, Model Reference Adaptive Control of Nonminimum Phase Milling", *Proceedings of 17th North American Manufacturing Research Conference*, Columbus, Ohio, pp. 266-273.

Ljung, L. and Söderström, T., 1983, *Theory and Practice of Recursive Identification*, Cambridge, Massachusetts: The MIT Press.

Ljung, L., 1987, *System Identification: Theory for the User*, Englewood Cliffs, New Jersey: Prentice Hall Inc.

Ljung, L., 1993, Identification of Linear Systems, *CAD for Control Systems*, D.A. Linkens, ed., New York: Marcel Dekker Inc., pp. 147-167.

Load Controls Inc., 1993, *PH-3A, PH-1000A Power Cell Power Transducer, Installation.*

Lozano, L.R. and Landau, I.D., 1982, Quasi-Direct Adaptive Control for Nonminimum Phase Systems, *ASME Journal of Dynamic Systems, Measurement, and Control*, V. 104, No.4, pp.311-316.

Ma, C.C.H. and Altintas, Y., 1990, Direct Adaptive Cutting Force Control of Milling Processes, *Automatica*, Vol. 26, No. 5, pp. 899-902.

Mandl, M., 1977, *Solid-State Circuit Design User's Manual*, Reston, Virginia: Reston Publishing Co., Inc.

Marshall, J.E., 1979, *Control of Time-Delay Systems*, Stevenage, UK: Peter Peregrinus Ltd.

Masory, O. and Koren, Y., 1980, Adaptive Control System for Turning, *Annals of CIRP*, Vol. 29, pp. 281-284.

Milner, D.A., 1975, Controller System Design for Feedrate Control by Deflection Sensing of a Machining Process, *International Journal of Machine Tool Design and Research*, Vol. 15, pp. 19-30.

Nasar, S.A. and Unnewehr, L.E., 1983, *Electromechanics and Electric Machines*, New York: John Wiley & Sons Inc.

Seborg. D.E., et al., 1989, *Process Dynamics and Control*, New York: John Wiley & Sons Inc.

Servo Products Inc., 1993, *2000/3000 Mill, System Operation and Programming*, Preliminary manual, Version 1.0.

Smith, S. and Tlusty, J., 1991, An Overview of Modelling and Simulation of the Milling Process, *ASME Journal of Engineering for Industry*, Vol. 113, pp. 169-175

Stein, J.L. and Wang, Churn-Hway, 1990, Analysis of Power Monitoring on AC Induction Drive Systems, *Journal of Dynamic Systems, Measurement, and Control*, Vol.112, pp.239-248.

Stute, G. and Goetz, F.R., Adaptive Control System for Variable Gain ACC Systems, *Proceedings of the 16th International Machine Tool Design and Research Conference*, 1976, pp. 117-121.

Tlusty, J., Cowley, A. and Elbestawi, M.A.A., 1978, A Study of An Adaptive Control System for Milling with Force Constraint, *6th North American Manufacturing Research Conference*, Gainesville, Florida, pp. 364-371.

Tlusty, J. and MacNeil, P., 1975, Dynamics of Cutting Forces in End Milling, *Annals of CIRP*, Vol. 24, pp. 21-25.

Tomizuka, M., Oh, J.H. and Dornfeld, D.A., 1983, Model Reference Adaptive Control of the Milling Process, *Control of Manufacturing Processes and Robotics Systems*, D.E. Hardt and W.J. Book, eds., ASME, New York, pp. 55-63.

Ulsoy, A.G. and Koren, Y., 1993, Control of Machining Processes, *Journal of Dynamic Systems, Measurement, and Control*, Vol. 115, pp. 301-308.

Ulsoy, A.G., Koren, Y. and Rasmussen, F., 1983, Principle Developments in the Adaptive Control of Machine Tools, *Journal of Dynamic Systems, Measurement, and Control*, Vol. 105, pp. 107-112.

Van den Bosch, P.P.J. and Van der Klauw, A.C., 1994, *Modelling, Identification and Simulation of Dynamical Systems*, Baca Raton, Florida: CRC Press.

Williams, A.B. and Taylor, F.J., 1988, *Electronic Filter Design Handbook: LC, Active, and Digital Filters*, New York: McGraw-Hill Publishing Co.

Zak, S.H. and Blouin, E.E., 1993, Ripple-Free Deadbeat Control, *IEEE Control Systems*, Vol. 13, No. 4, pp. 51-56.

Zorbas, D., 1989, *Electric Machines: Principles, Applications and Control Schematics*, West Publishing Co.

Appendix A

Technical Data and Configuration of Experimental Equipments

A.1 Technical Data of Load Controls PH-3A (230V 10A 0~10V) Power Cell Power Sensor

A.2 Technical Data of 3-Component Dynamometer Type 9257B (excerpt)

A.3 Technical Data of Kistler Dual Mode Amplifier Type 5010A (excerpt)

A.4 Configuration of Kistler Dual Mode Amplifier Type 5010A

A.1 Technical Data of Load Controls PH-3A (230V 10A 0~10V) Power Cell Power Sensor

Full scale capacity	5HP
Frequency	3 Hz to 1 kHz (derate above 1 kHz)
Response	15 milliseconds (0.015 seconds) 0.060 seconds to 1 second with optional response adjustment
Accuracy/Repeatability	2.5% of Full Scale 0.25%

Compliance/Impedance

Compliance: 6 Volts
10 Volt output: 2K ohm minimum connected impedance
4 - 20 MA output: 300 ohm maximum connected impedance

A.2 Technical Data of 3-Component Dynamometer Type 9257B (excerpt)

Force application within and max. 25 m above top surface	Fx, Fy, Fz	kN	-5 ... 5
Overload	Fx, Fy, Fz	kN	-7.5/7.5
with Fx and Fy $\leq$0.5 Fz	Fz	kN	-7.5/15
Response threshold		N	<0.01
Sensitivity (all ranges)	Fx, Fy	pC/N	-7.97
(from the calibration sheets)	Fz	pC/N	-3.8
Linearity (all ranges) (from the calibration sheets)		%FSO	$\leq \pm$0.3
Rigidity	cx, cy	kN/μm	>1
	cz	kN/μm	>2
Natural frequency	f_0(x,y,z)	kHz	$\approx$3.5

A.3 Technical Data of Kistler Dual Mode Amplifier Type 5010 (excerpt)

Measuring range (Charge mode)	mV	$\pm$ 10 to 999000
Transducer sensitivity	pC/MU or mv/MU	0.01 to 9990.0
Scale	MU/V	0.0002 to 10M
Accuracy	%	$\leq$0.5

Time constant	seconds	Long: up to 100000 Medium: 1 to 10000 Short: 0.01 to 100
Filter, with standard low-pass		
Filter type		One pole passive
Cut-off frequency (-3dB)	Hz	180K
Frequency accuracy	%	±10
Input voltage, max value for pulse widths ≤ 3	V	±50
Output		
Impedance	Ω	100
Voltage range	V	±10
Current Limit	mA	±5

A.4 Configuration of the Kistler Dual Mode Amplifier Type 5010

Mode	Charge
Time constant	Medium
Transducer sensitivity	7.97 pC/MU for x and y axes
Scale	500 MU/Volt
Low-pass filter	Standard (180 kHz)